

# Explicit expressions for prestack map time migration in isotropic and VTI media and the applicability of map depth migration in heterogeneous anisotropic media

Huub Douma<sup>1</sup> and Maarten V. de Hoop<sup>1</sup>

## ABSTRACT

We present 3D prestack map time migration in closed form for qP-, qSV-, and mode-converted waves in homogeneous transversely isotropic media with a vertical symmetry axis (VTI). As far as prestack time demigration is concerned, we present closed-form expressions for mapping in homogeneous isotropic media, while for homogeneous VTI media we present a system of four nonlinear equations with four unknowns to solve numerically. The expressions for prestack map time migration in VTI homogeneous media are directly applicable to the problem of anisotropic parameter estimation (i.e., the anellipticity parameter  $\eta$ ) in the context of time-migration velocity analysis. In addition, we present closed-form expressions for both prestack map time migration and demigra-

tion in the common-offset domain for pure-mode (P-P or S-S) waves in homogeneous isotropic media that use only the slope in the common-offset domain as opposed to slopes in both the common-shot and common-receiver (or equivalently the common-offset and common-midpoint) domains. All time-migration and demigration equations presented can be used in media with mild lateral and vertical velocity variations, provided the velocity is replaced with the local rms velocity. Finally, we discuss the condition for applicability of prestack map depth migration and demigration in heterogeneous anisotropic media that allows the formation of caustics and explain that this condition is satisfied if, given a velocity model and acquisition geometry, one can map-depth-migrate without ambiguity in either the migrated location or the migrated orientation of reflectors in the image.

## INTRODUCTION

The geometry of seismic migration can be understood and described in terms of surfaces of equal traveltime, i.e., isochrons. Migration integrates signal-processed data along diffraction surfaces related to these isochrons. In terms of linear filter theory, in homogeneous media the image is a convolution of the impulse response, shaped in accordance with the isochrons of the migration operator, with the data. This approach uses the positions, traveltimes, and amplitudes of the events in the data and thus only implicitly uses the information given by the reflection slopes.

In the high-frequency approximation, seismic waves (or wave singularities) propagate along rays through the subsurface. Provided the velocity in the earth is known, reflection slopes in the data determine the directions of such rays at the recording surface (or the singular direction of the wavefront set of the recorded wavefield). Therefore, once the traveltime

and the slopes at the source and receiver are known along with the velocity, the location and local dip of a subsurface reflector (or image singularity) can in principle be determined with the aid of numerical ray tracing (Červený, 2001).

The determination of the reflector position and orientation from the times and slopes of zero-offset reflection seismic data is generally referred to as map migration (Kleyn, 1977). Determination from times and slopes of reflection data at the source and receiver locations is called prestack map migration. In a mathematical context, provided the velocity is known and the medium does not allow different reflectors to have identical surface seismic measurements that persist under small perturbations of the reflectors, the use of the slope information results in a one-to-one mapping from the unmigrated quantities associated with a reflection in the data (given a scattering angle and azimuth) to the migrated quantities associated with a reflector in the image. Collecting the migrated and unmigrated quantities in a table leads to the notion of canonical relation.

Manuscript received by the Editor June 17, 2003; revised manuscript received April 1, 2005; published online January 12, 2006.

<sup>1</sup>Colorado School of Mines, Center for Wave Phenomena, 1500 Illinois St., Golden, Colorado 80401. E-mail: huub@dix.mines.edu; mdehoop@dix.mines.edu.

© 2006 Society of Exploration Geophysicists. All rights reserved.

Here we attempt to show that prestack map depth migration and demigration are closely related to the canonical relation of the single scattering imaging or modeling operators in complex media. Imaging artifacts (or imaging phantoms) are avoided if the projection of this canonical relation on the unmigrated quantities is one-to-one. This condition was introduced by Guillemin (1985) and further exploited by ten Kroode et al. (1998), de Hoop and Brandsberg-Dahl (2000), and Stolk and de Hoop (2001). We explain that this is precisely the applicability condition that allows map depth migration in inhomogeneous anisotropic media (i.e., in the presence of caustics).

The concept of map migration is certainly not new. Weber (1955) gives an early account of map migration, wherein the zero-offset 3D map migration equations are derived for a constant-velocity medium and arbitrary recording surface. Independently, Graeser et al. (1957) and Haas and Viallix (1976) use the slopes in the data to derive the position of a reflector in three dimensions from zero-offset data for a homogeneous isotropic medium. In an early attempt at the use of numerical ray tracing, Musgrave (1961) uses slope information to calculate wavefront charts and migration-table lists, and Sattlegger (1964) derives a series expansion for the coordinates of the raypath that uses the slopes in the data. Both methods assume vertically varying velocity media and can be used for 3D migration of zero-offset data. Reilly (1991) and Whitcombe and Carroll (1994) present successful applications of poststack map migration on field data.

Map migration has been used for velocity estimation in several different approaches [e.g., Gjoystdal and Ursin (1981), Gray and Golden (1983), and Maher et al. (1987)]. To improve horizon-based velocity model building, map migration has been used in seismic event-picking schemes consisting of map migration, followed by picking of events and slopes, map demigration, and remigration in the updated velocity model. The initial map-migration step in such a scheme attempts to reduce mispositioning of the velocity picks. The idea to use map migration for velocity analysis stems from the sensitivity of prestack map migration to the migration velocity model, as pointed out by Sattlegger et al. (1980). Sword (1987, p. 22) develops a controlled directional reception (CDR) tomographic inversion technique, first suggested by Harlan and Burrige (1983), to find interval velocities from prestack seismic data. In this method the slopes (or horizontal slownesses) are picked automatically using the CDR picking technique — slant stack over a short range of offsets with subsequent picking — developed in the former Soviet Union [e.g., Zavalishin (1981) and Riabinkin (1991)] but first introduced by Rieber (1936) and later reintroduced by Hermont (1979). Subsequently, the estimates of the ray parameters are used to trace rays through the initial estimate of the velocity model, and a depth is found wherein the sum of the traveltimes along the downgoing (source) and upgoing (receiver) rays equals the observed traveltimes. Then, at this depth, the horizontal distance between the endpoints of two subsurface rays is minimized using a modified Gauss-Newton method to yield the velocity model.

Iversen and Gjoystdal (1996) have performed 2D map migration in arbitrarily complex media using a layer-stripping approach similar to that of Gray and Golden (1983) to achieve

simultaneous inversion of velocity and reflector structure; they have extended this method to 2D anisotropic media (Iversen et al., 2000). Their linearized inversion scheme, which minimizes the projected difference along the reflector normal between events from different offsets, uses derivatives of reflection-point coordinates with respect to model parameters as introduced by van Trier (1990) rather than derivatives of traveltimes with respect to model parameters as used in classical tomographic inversion (e.g., Bishop et al., 1985). Such an approach allows for more consistent event picking because reflectors can be identified in a geological structure. In addition, an initial imaging step generally improves the S/N ratio, allowing for more accurate event picking. Finally, Billette and Lambaré (1998) reiterate the importance of slope information in velocity-model estimation while validating that precision in measured slopes, traveltimes, and positions in seismic reflection data is sufficient to recover velocities using stereotomography.

In this paper we first develop closed-form expressions for the geometry of prestack map time migration and demigration in three dimensions for a homogeneous isotropic medium. These migration equations assume, in addition to the velocity (as is common in seismic imaging), that only the location and the slopes in unmigrated common-offset gathers are known. This is in contrast to the 2D migration equations presented by Sword (1987, p. 22), which also require the slope within the common-midpoint (CMP) gathers (or, alternatively, the slopes in the common-source and common-receiver gathers). Time migration, which uses the assumption of an rms velocity, remains in use. In this context our expressions have current applicability, provided the constant velocity in them is replaced by the local rms velocity. To complement the work of Alkhalifah and Tsvankin (1995) and Alkhalifah (1996) on velocity analysis in transversely isotropic (TI) media, we derive closed-form expressions for 3D prestack map time migration for qP-waves, qP-qSV mode-converted waves, and qSV-waves in transversely isotropic media with a vertical symmetry axis (VTI). These expressions are directly applicable to the problem of anisotropic parameter estimation (such as the anellipticity parameter  $\eta$ ) in the context of time-migration velocity analysis.

For 3D prestack map time demigration in such media, we present a system of four nonlinear equations with four unknowns that needs to be solved numerically. Since in the vertical symmetry plane of TI media with a tilted symmetry axis (TTI) the phase and group directions are both in this plane our results apply also to the vertical symmetry plane of homogeneous TTI media. Furthermore, the kinematic equivalence of TI media and orthorhombic media in the symmetry planes generalizes our results to these planes in orthorhombic media. We then proceed to explain the applicability of map depth migration in heterogeneous anisotropic media and revisit prestack map time migration in homogeneous isotropic media to show that the prestack map time migration and demigration equations define the canonical relation of the single-scattering modeling and imaging operators in such media. For practical issues such as slope estimation, accuracy and stability of the algorithm, and sampling and grid distortion, we refer to the existing literature [e.g., Kleyn (1997); Maher and Hadley (1985)].

### MAP TIME MIGRATION AND DEMIGRATION IN ISOTROPIC MEDIA

To illustrate the concept of map migration, we derive explicit 3D prestack map migration and demigration equations for isotropic homogeneous media. We assume that preprocessing has already compensated data for any topography on the acquisition surface and deal with only the geometry of migration. The results, however, could be extended to take geometrical spreading effects into account. For media with mild lateral and vertical velocity variations, these equations can be used, provided the velocity is replaced with the local rms velocity.

For 2D prestack map time migration, Sword (1987, p. 22) derives closed-form expressions for the migrated location and reflector dip using the horizontal slownesses at both the source and the receiver. It turns out, however, that for prestack map time migration and demigration in homogeneous isotropic media, we do not need the angles at the source and the receiver given by the horizontal slownesses. We demonstrate this by deriving closed-form expressions for pre-stack map time migration and demigration in three dimensions that use only the slopes in common-offset gathers. These expressions provide a practical advantage over existing closed-form solutions that use both slownesses, since only one slope needs to be measured instead of two. Unfortunately, such a reduction no longer holds in heterogeneous or anisotropic media.

#### The double-square-root equation

The double-square-root (DSR) equation governing traveltime in a homogeneous isotropic medium in three dimensions is given by

$$t_u = \frac{1}{v} \left( \sqrt{(\tilde{x}_u - \tilde{x}_m - h \sin \alpha)^2 + (\tilde{y}_u - \tilde{y}_m - h \cos \alpha)^2 + \left(\frac{vt_m}{2}\right)^2} + \sqrt{(\tilde{x}_u - \tilde{x}_m + h \sin \alpha)^2 + (\tilde{y}_u - \tilde{y}_m + h \cos \alpha)^2 + \left(\frac{vt_m}{2}\right)^2} \right), \quad (1)$$

where  $\tilde{x}_u$  and  $\tilde{y}_u$  are the CMP coordinates,  $\tilde{x}_m$  and  $\tilde{y}_m$  are the reflection-point coordinates,  $t_m$  is the two-way migrated traveltime,  $\alpha$  is the acquisition azimuth measured positive in the direction of the positive  $\tilde{x}$ -axis,  $v$  is the velocity, and  $h$  is the half-offset (see Figure 1). Here, we consider only pure modes, i.e., P-P or S-S reflections, since the velocity at the source and receiver are assumed to be equal; however, the case of mode-converted waves should be a straightforward generalization of the approach outlined in this section.

Rotating the positive  $\tilde{y}$ -direction to the source-to-receiver direction, the DSR equation becomes

$$t_u = \frac{1}{v} \left( \sqrt{(x_u - x_m)^2 + (y_u - y_m - h)^2 + \left(\frac{vt_m}{2}\right)^2} + \sqrt{(x_u - x_m)^2 + (y_u - y_m + h)^2 + \left(\frac{vt_m}{2}\right)^2} \right). \quad (2)$$

To find  $x_u, y_u, t_u, p_u^x$ , and  $p_u^y$  from  $\tilde{x}_u, \tilde{y}_u, t_u, \tilde{p}_u^x$ , and  $\tilde{p}_u^y$ , where  $p_u^x, p_u^y$  and  $\tilde{p}_u^x, \tilde{p}_u^y$  are the horizontal slownesses of the unmigrated reflection in the rotated and unrotated coordinate systems, respectively, we use

$$\begin{pmatrix} x_u \\ y_u \\ t_u \\ p_u^x \\ p_u^y \end{pmatrix} = \begin{pmatrix} \cos \alpha & \sin \alpha & 0 & 0 & 0 \\ -\sin \alpha & \cos \alpha & 0 & 0 & 0 \\ 0 & 0 & 1 & 0 & 0 \\ 0 & 0 & 0 & \cos \alpha & -\sin \alpha \\ 0 & 0 & 0 & \sin \alpha & \cos \alpha \end{pmatrix} \begin{pmatrix} \tilde{x}_u \\ \tilde{y}_u \\ t_u \\ \tilde{p}_u^x \\ \tilde{p}_u^y \end{pmatrix}. \quad (3)$$

To be consistent with the general treatment of time migration using CMP coordinates and offset, we derive our results in this reference frame. Since we align the positive y-axis with

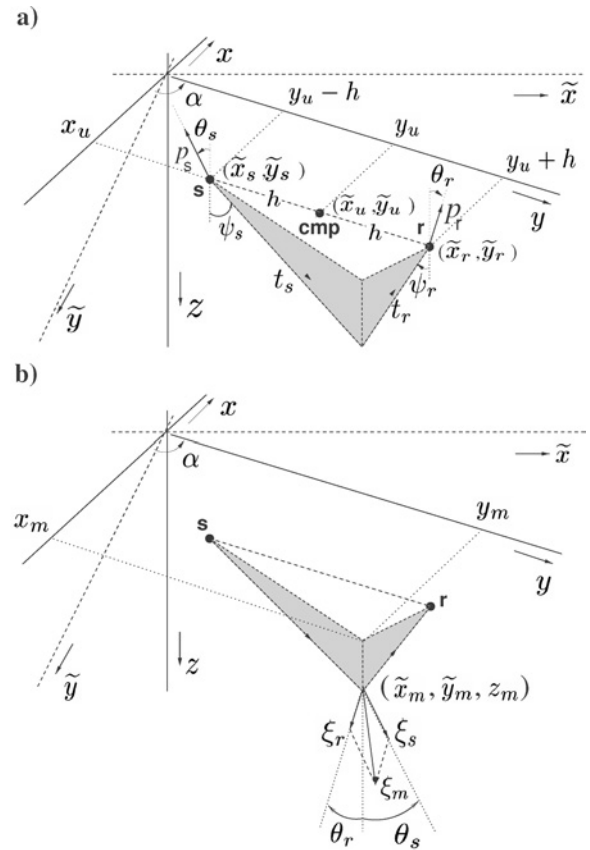


Figure 1. Geometry defining the DSR equation for a VTI medium in both the unrotated  $(\tilde{x}, \tilde{y})$  and rotated  $(x, y)$  reference frames. (a) Coordinates describing the data: source location  $(\tilde{x}_s, \tilde{y}_s)$  or  $(x_s = x_u, y_s = y_u - h)$  with  $h$  the half-offset, receiver location  $(\tilde{x}_r, \tilde{y}_r)$  or  $(x_r = x_u, y_r = y_u + h)$ , midpoint location  $(\tilde{x}_u, \tilde{y}_u)$  or  $(x_u, y_u)$ , two-way traveltime  $t_u = t_s + t_r$ , and the slowness vectors at the source  $(\mathbf{p}_s)$  and receiver  $(\mathbf{p}_r)$ . The values  $\theta_{s,r}$  and  $\psi_{s,r}$  are, respectively, the phase and group angles with the vertical symmetry axis at the source  $s$  and receiver  $r$ . The angle  $\alpha$  is the angle between the  $\tilde{y}$ - and  $y$ -directions, i.e., the acquisition azimuth. (b) Coordinates describing the image: the migrated location  $(\tilde{x}_m, \tilde{y}_m, z_m)$  or  $(x_m, y_m, z_m)$  with (for qP-waves)  $z_m = V_{p0}t_m/2$  and  $t_m$  the migrated two-way traveltime, the wave vectors  $\xi_s$  and  $\xi_r$  from the source  $s$  and receiver  $r$ , and the wave vector associated with the reflector  $\xi_m$  (i.e., the dip covector).

the source-to-receiver direction, we develop our equations in the common-offset, common-azimuth domain. In the remaining text we assume the velocity to be known and equal to the rms velocity, i.e., we develop the prestack map migration and demigration equations and their solutions in the context of time migration. Table 1 summarizes our notation throughout the remaining text.

### Prestack common-offset migration

Equation 2 has three unknowns:  $x_m$ ,  $y_m$ , and  $t_m$ . We obtain two additional equations by calculating the partial derivatives of  $t_u$  with respect to  $x_u$  and  $y_u$  while keeping the reflector location and offset constant, i.e.,  $p_u^x = 1/2(\partial t_u/\partial x_u)$  and  $p_u^y = 1/2(\partial t_u/\partial y_u)$ :

$$p_u^x = \frac{1}{2v} \left( \frac{x_u - x_m}{\sqrt{(x_u - x_m)^2 + (y_u - y_m - h)^2 + \left(\frac{vt_m}{2}\right)^2}} + \frac{x_u - x_m}{\sqrt{(x_u - x_m)^2 + (y_u - y_m + h)^2 + \left(\frac{vt_m}{2}\right)^2}} \right), \quad (4)$$

**Table 1. Summary of notation.**

Variable	Description
$h$	Half-offset
$p^{x,y}$	Horizontal slowness in $x$ - or $y$ -direction
$s, r$	Subscripts denoting source ( $s$ ) and receiver ( $r$ ) variables
$(s, r)_\gamma$	$(\sin \gamma_s, \sin \gamma_r)$
$(s, r)_\theta$	$(\sin \theta_s, \sin \theta_r)$
$t_{s,r}$	One-way traveltimes from source ( $s$ ) or receiver ( $r$ ) to reflection point
$t_{u,m}$	Two-way unmigrated ( $u$ ) and migrated ( $m$ ) traveltimes
$u, m$	Subscripts denoting migrated ( $m$ ) and unmigrated ( $u$ ) variables
$v$	Group velocity
$V$	Phase velocity
$V_{\text{NMO}}(0)$	Zero-dip NMO velocity
$V_{p0,s0}$	Vertical phase velocity for qP- and qSV-waves, respectively
$x, y, z$	Horizontal location $x$ and $y$ and depth $z$
$\alpha$	Acquisition azimuth (measured counterclockwise with positive $y$ -axis)
$\gamma$	Azimuth angle of slowness vector with positive $x$ -axis (clockwise positive)
$\epsilon, \delta$	Thomsen parameters
$\eta$	Anellipticity parameter
$\theta$	Phase angle
$v_{x,y}$	$-\tan \phi_{x,y}$
$\tilde{\mathbf{x}}_m$	Dip covector (i.e., the wave vector associated with the reflector in the image)
$\phi_{x,y}$	Reflector dip angle with horizontal in $x$ or $y$ direction
$\psi$	Group angle

$$p_u^y = \frac{1}{2v} \left( \frac{y_u - y_m - h}{\sqrt{(x_u - x_m)^2 + (y_u - y_m - h)^2 + \left(\frac{vt_m}{2}\right)^2}} + \frac{y_u - y_m + h}{\sqrt{(x_u - x_m)^2 + (y_u - y_m + h)^2 + \left(\frac{vt_m}{2}\right)^2}} \right), \quad (5)$$

where the horizontal slownesses  $p_u^x$  and  $p_u^y$  can be measured. With these additional equations we arrive at a system of three equations with three unknowns. To derive equations 4 and 5, we use the property that on the prestack migration isochron, defined by the DSR equation,  $\partial t_m/\partial x_u = \partial t_m/\partial y_u = 0$  for constant  $h$ .

Solving equations 2, 4, and 5 for  $x_m$ ,  $y_m$ , and  $t_m$  results in

$$x_m = x_u - \frac{v^2 p_u^x t_u}{2} (1 - \Lambda_u^2), \quad (6)$$

$$y_m = y_u - \left(\frac{vt_u}{2}\right)^2 \frac{\Lambda_u}{h}, \quad (7)$$

$$t_m = 2 \left\{ \left(\frac{t_u}{2}\right)^2 (1 - (vp_u^x)^2) - \left(\frac{h}{v}\right)^2 + \left(\frac{vt_u \Lambda_u}{4h}\right)^2 \times \left( 8 (p_u^x h)^2 - t_u^2 + \left(\frac{2h}{v}\right)^2 [1 - (vp_u^x \Lambda_u)^2] \right) \right\}^{\frac{1}{2}}, \quad (8)$$

in which

$$\Lambda_u = \Lambda_u(p_u^y, \Theta_u, h) \equiv \frac{1}{2\sqrt{2}p_u^y h} \sqrt{\Theta_u \left( 1 - \sqrt{1 - \frac{64 (p_u^y h)^4}{\Theta_u^2}} \right)} \quad (9)$$

with

$$\Theta_u = \Theta_u(t_u, p_u^y, h) \equiv t_u^2 + \left(\frac{2h}{v}\right)^4 \frac{1}{t_u^2} - 2 \left(\frac{2h}{v}\right)^2 (1 - (vp_u^y)^2). \quad (10)$$

The signs of the roots are chosen such that migration moves energy updip. The local dip of the reflector  $p_m^{x,y} = 1/2(\partial t_m/\partial(x, y)_m)$  can be found by calculating the partial derivatives  $(\partial/\partial x_m, \partial/\partial y_m)$  of equation 2, using  $(\partial t_u/\partial x_m) = (\partial t_u/\partial y_m) = 0$  for constant  $h$  and using equations 6–8 for  $x_m$ ,  $y_m$ , and  $t_m$ . This yields

$$p_m^{x,y} = \frac{1}{2} p_u^{x,y} t_u |\Lambda_u - 1| |\Lambda_u + 1| \times \left\{ \left(\frac{t_u}{2}\right)^2 (1 - (vp_u^x)^2) - \left(\frac{h}{v}\right)^2 + \left(\frac{vt_u \Lambda_u}{4h}\right)^2 \times \left( 8 (p_u^x h)^2 - t_u^2 + \left(\frac{2h}{v}\right)^2 (1 - (vp_u^x \Lambda_u)^2) \right) \right\}^{-\frac{1}{2}}. \quad (11)$$

Equations 6–8 and 11 thus are explicit expressions that determine the migrated reflector coordinates  $(x_m, y_m, t_m, p_m^x, p_m^y)$  from the specular reflection coordinates  $(x_u, y_u, t_u, p_u^x, p_u^y)$ , given  $h$  and  $v$ . Setting  $x_m = x_u = 0$  and  $p_m^x = p_u^x = 0$  reduces equations 7, 8, and 11 to the 2D equivalent expressions.

Note that equations 6–8 and 11 do not use the offset horizontal slowness  $p_h = 1/2(\partial t_u/\partial h)$ . This means that, in practice, only  $p_u^x$  and  $p_u^y$  need to be estimated and the slope in a CMP gather can be ignored. Usually expressions or algorithms for map migration use the slopes in both the common-offset and CMP gathers or, alternatively, the slopes in source and receiver gathers.

### Zero-offset migration

Equations 6–8 and 11 seem to be singular at first sight for  $h = 0$  and  $p_u^h = 0$ , and they are valid strictly when  $h \neq 0$  and  $p_u^y \neq 0$ . However, these singularities are introduced in the derivation of these expressions through division by  $h$  and  $p_u^y$ . For small  $h$  or  $p_u^y$ , i.e.,  $64(p_u^y h)^4/\Theta_u^2 \ll 1$ , we use a first-order Taylor expansion for  $\Lambda_u$  such that

$$\Lambda_u \simeq \frac{2p_u^y h}{\sqrt{\Theta_u}}. \quad (12)$$

Substituting this approximation for  $\Lambda_u$  into equations 6–8 and 11 gives

$$x_m \simeq x_u - \frac{v^2 p_u^x t_u}{2} \left( 1 - \frac{4(p_u^y h)^2}{\Theta_u} \right), \quad (13)$$

$$y_m \simeq y_u - \frac{(vt_u)^2 p_u^y}{2\sqrt{\Theta_u}}, \quad (14)$$

$$t_m \simeq 2 \left\{ \frac{t_u^2}{4} (1 - (vp_u^x)^2) - \left( \frac{h}{v} \right)^2 + \frac{1}{\Theta_u} \left( \frac{vt_u p_u^y}{2} \right)^2 \left( 8(p_u^x h)^2 - t_u^2 + \left( \frac{2h}{v} \right)^2 \times \left[ 1 - \frac{1}{\Theta_u} (2vp_u^x p_u^y h)^2 \right] \right) \right\}^{\frac{1}{2}}, \quad (15)$$

$$p_m^{x,y} \simeq \frac{1}{2} p_u^{x,y} t_u \times \left| \frac{2p_u^y h}{\sqrt{\Theta_u}} - 1 \right| \left| \frac{2p_u^y h}{\sqrt{\Theta_u}} + 1 \right| \left\{ \left( \frac{t_u^2}{4} (1 - (vp_u^x)^2) - \left( \frac{h}{v} \right)^2 \right) + \frac{1}{\Theta_u} \left( \frac{vt_u p_u^y}{2} \right)^2 \left( 8(p_u^x h)^2 - t_u^2 + \left( \frac{2h}{v} \right)^2 \left[ 1 - \frac{1}{\Theta_u} (2vp_u^x p_u^y h)^2 \right] \right) \right\}^{-\frac{1}{2}}. \quad (16)$$

For the special case when  $h = 0$ , these equations reduce to their zero-offset (or poststack) counterparts, i.e.,

$$(x, y)_m = (x, y)_u - \frac{v^2 p_u^{x,y} t_u}{2}, \quad (17)$$

$$t_m = t_u \sqrt{1 - v^2 p_u^2}, \quad (18)$$

$$p_m^{x,y} = \frac{p_u^{x,y}}{\sqrt{1 - v^2 p_u^2}}, \quad (19)$$

where

$$p_u \equiv \sqrt{(p_u^x)^2 + (p_u^y)^2}. \quad (20)$$

Equations 17 and 18 can also be found in Haas and Viallax (1976); note the typographical error in their equations for the migrated location. Setting  $x_m = x_u = 0$  and  $p_m^x = p_u^x = 0$  gives the expressions in two dimensions. These 2D expressions can also be found in Claerbout (1985, chapter 1).

### Prestack common-offset demigration

The demigration equations for  $x_u$  and  $y_u$  can be found by first solving equation 2 for  $t_m$  and evaluating the partial derivatives  $(\partial t_m/\partial x_m)$  and  $(\partial t_m/\partial y_m)$ . Using the resulting expressions for  $x_u$  and  $y_u$  in equation 2 then gives the explicit expression for  $t_u$ . To find the slopes  $p_u^x$  and  $p_u^y$ , we then substitute the expressions for  $x_u, y_u$ , and  $t_u$  in equations 4 and 5. The resulting equations are

$$x_u = x_m + \frac{v^2 p_m^x t_m}{2}, \quad (21)$$

$$y_u = y_m + \frac{v^2 p_m^y t_m}{2} + h \Lambda_m, \quad (22)$$

$$t_u = \sqrt{\frac{4h^2}{v^2} + \frac{2p_m^y h t_m}{\Lambda_m}}, \quad (23)$$

$$p_u^{x,y} = \frac{p_m^{x,y} t_m}{|\Lambda_m - 1| |\Lambda_m + 1| \sqrt{\frac{4h^2}{v^2} + \frac{2p_m^y h t_m}{\Lambda_m}}}, \quad (24)$$

in which

$$\Lambda_m = \Lambda_m(p_m^y, \Theta_m, h) \equiv \frac{4p_m^y h}{\Theta_m \left( 1 + \sqrt{1 + \frac{16(p_m^y h)^2}{\Theta_m^2}} \right)}, \quad (25)$$

with

$$\Theta_m = \Theta_m(t_m, p_m^{x,y}) \equiv t_m \left( 1 + v^2 \left[ (p_m^x)^2 + (p_m^y)^2 \right] \right). \quad (26)$$

Equations 21–24 determine the specular reflection  $(x_u, y_u, t_u, p_u^x, p_u^y)$  from the reflector  $(x_m, y_m, t_m, p_m^x, p_m^y)$ . Note that  $p_m^{x,y}$  can be estimated from the dip of the imaged reflector using

$$\tan \phi_{x,y} = \frac{v}{2} \frac{\partial t_m}{\partial (x, y)_m} = vp_m^{x,y}, \quad (27)$$

where  $\phi_{x,y}$  is the reflector dip angle with the horizontal in the  $x$ - or  $y$ -direction (measured positive clockwise). Again, the 2D case follows by setting  $x_m = x_u = 0$  and  $p_m^x = p_u^x = 0$ .

### Zero-offset demigration

The demigration mapping given by equations 21–24 indeed reduces to its zero-offset counterpart if  $h = 0$ . The resulting

expressions are

$$(x, y)_u = (x, y)_m + \frac{v^2 p_m^{x,y} t_m}{2}, \quad (28)$$

$$t_u = t_m \sqrt{1 + v^2 p_m^2}, \quad (29)$$

$$p_u^{x,y} = \frac{p_m^{x,y}}{\sqrt{1 + v^2 p_m^2}}, \quad (30)$$

where

$$p_m \equiv \sqrt{(p_m^x)^2 + (p_m^y)^2}. \quad (31)$$

With  $x_m = x_u = 0$  and  $p_m^x = p_u^x = 0$ , these expressions reduce to the 2D case.

### Numerical example

Figures 2a and 2b show modeled common-offset reflection seismic data from a syncline reflector, embedded in a constant-velocity medium with  $v = 2000$  m/s, and its migrated counterpart, respectively; the offset is 2000 m (i.e.,  $h = 1000$  m). To verify the prestack map migration and demigration equations numerically, Figures 2c and 2d show line elements overlaid on the common-offset data and the migrated data, respectively. The line elements in Figure 2c were obtained using points along the syncline in our model (giving  $y_m$  and  $t_m$ ) and the associated local dips at these points. These dips were converted to migrated horizontal slowness (i.e.,  $p_m^y$ ) using equa-

tion 27, and the values of  $y_u$ ,  $t_u$ , and  $p_u^y$ , i.e., the demigrated variables, were found using the 2D equivalent expressions of equations 22–24 (i.e., with  $p_m^x = 0$ ). To find the line elements associated with the diffractions from the edges of the syncline, we took a fan of line elements centered at these edges, with a range of dips from  $-80^\circ$  to  $80^\circ$ , and demigrated them according to the procedure just described. Figure 2c shows excellent agreement between the line elements and the data, indicating the validity of the common-offset map time-demigration equations 21–24.

The values of  $y_u$ ,  $t_u$ , and  $p_u^y$  thus obtained were subsequently used in equations 7, 8, and 11 (with  $p_u^x = 0$ ) to calculate the migrated counterparts  $y_m$ ,  $t_m$ , and  $p_m^y$ . The obtained values for  $p_m^y$  were converted to local reflector dip using equation 27, giving the orientations of the line elements shown in Figure 2d. The resulting line elements coincide with the migrated data, indicating the validity of the common-offset map time migration equations 6–8 and 11. Note how the line elements from the diffractions (indicated by the dark gray line elements) associated with the edges of the syncline-shaped reflector are all map migrated to the same location but with different orientations, much like the Fourier transform of a delta function in space has all  $\mathbf{k}$ -directions.

### MAP TIME MIGRATION AND DEMIGRATION IN VTI MEDIA

We consider now the case of homogeneous VTI media. In our derivation, we incorporate the fact that in such media the phase and group velocity vectors lie in the vertical plane. Since for homogeneous TTI media this requirement is also satisfied in the vertical symmetry plane that contains the symmetry axis, our results also apply to this plane in homogeneous TTI media. Furthermore, the kinematic equivalence of TI media and orthorhombic media in the symmetry planes generalizes our results to these planes in orthorhombic media.

### The DSR equation

In general, the group velocity vector is perpendicular to the slowness surface, whereas the slowness vector is perpendicular to the wavefront. In TI media, the group velocity  $v$  depends only on the phase angle  $\theta$  with the axis of rotational symmetry and is given by (Tsvankin, 2001, p. 29)

$$v = V(\theta) \sqrt{1 + \left( \frac{1}{V(\theta)} \frac{dV}{d\theta} \right)^2}, \quad (32)$$

where  $V$  is the phase velocity of either qP- or qSV-waves. The group angle  $\psi$  in such media follows from

$$\tan \psi = \frac{\tan \theta + \frac{1}{V(\theta)} \frac{dV}{d\theta}}{1 - \frac{\tan \theta}{V(\theta)} \frac{dV}{d\theta}}. \quad (33)$$

The group angle  $\psi$  is defined as the angle of the ray with the rotational symmetry axis, while the phase angle  $\theta$  is the angle of the normal to the wavefront with the symmetry axis (see Figure 1a). Energy travels along a ray with the group velocity, so the DSR equation for a homogeneous anisotropic medium

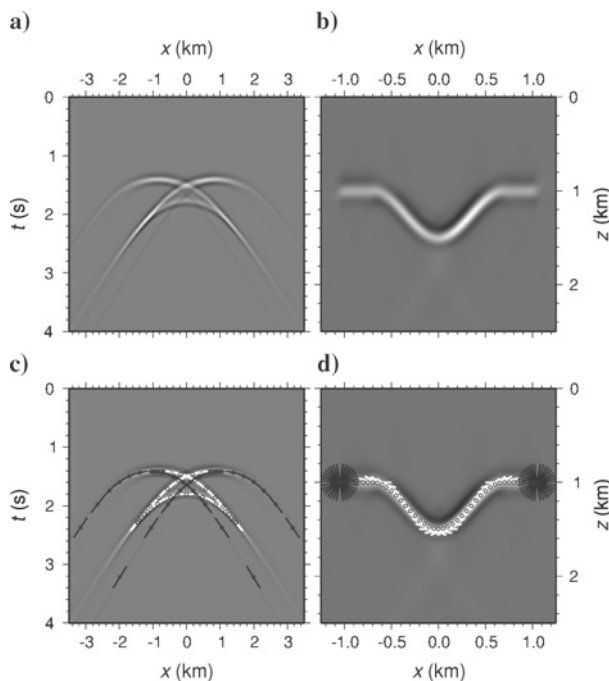


Figure 2. (a) Common-offset ( $h = 1000$  m) data and (b) migrated data from a syncline-shaped reflector embedded in a constant-velocity ( $v = 2000$  m/s) medium. (c) Demigrated and (d) migrated line elements superimposed on the data and migrated data, respectively. The excellent agreement between the demigrated line elements and the seismic data (c) and the migrated line elements and the image (d) indicate the validity of the common-offset map time demigration and migration equations, respectively.

is given by

$$t_u = \frac{\sqrt{(x_{s,r} - x_m)^2 + (y_s - y_m)^2 + z_m^2}}{v_s} + \frac{\sqrt{(x_{s,r} - x_m)^2 + (y_r - y_m)^2 + z_m^2}}{v_r}, \quad (34)$$

where  $v_{s,r}$  are the group velocities in the directions of the rays connecting the source with the reflection point and the receiver with the reflection point, respectively;  $(x_{s,r}, y_{s,r})$  are the source and receiver coordinates. The positive  $y$ -direction is in the source-to-receiver direction (i.e.,  $x_{s,r} = x_u$ ), and the coordinate system is right-handed as before (see Figure 1a). Note that  $v_{s,r}$  could be the group velocity for either qP- or qSV-waves.

### Medium parameterization

For general TI media, the phase velocity for qP- and qSV-waves using the parameterization introduced by Thomsen (1986) is given by (Tsvankin, 2001, p. 22)

$$V(\theta) = V_{P0} \sqrt{1 + \epsilon \sin^2 \theta - \frac{f}{2} \pm \frac{f}{2} \sqrt{\left(1 + \frac{2\epsilon \sin^2 \theta}{f}\right)^2 - \frac{2(\epsilon - \delta) \sin^2 2\theta}{f}}}, \quad (35)$$

where  $V_{P0}$  is the phase velocity for the qP-wave at  $\theta = 0$ ,  $f \equiv 1 - (V_{S0}^2/V_{P0}^2)$  where  $V_{S0}$  is the phase velocity of the qSV-wave at  $\theta = 0$ , and  $\epsilon$  and  $\delta$  are the Thomsen anisotropy parameters. The plus sign refers to qP-waves, and the minus sign refers to qSV-waves. Taking the derivative with respect to the phase angle  $\theta$  gives

$$\frac{dV}{d\theta} = \frac{V_{P0}^2}{V(\theta)} \left( \epsilon s \sqrt{1 - s^2} \pm \frac{\left(1 + \frac{2\epsilon s^2}{f}\right) \epsilon s \sqrt{1 - s^2} - 2(\epsilon - \delta) s \sqrt{1 - 5s^2 - 4s^6}}{\sqrt{\left(1 + \frac{2\epsilon s^2}{f}\right)^2 - \frac{8(\epsilon - \delta) s^2 (1 - s^2)}{f}}} \right), \quad (36)$$

where  $s \equiv \sin \theta$ . Again, the plus sign refers to qP-waves and the minus sign refers to qSV-waves. Note that we have  $0 \leq \theta < \pi/2$ , since rays cannot turn in homogeneous media.

The qP-wave phase velocity, however, depends only weakly on the vertical shear-wave velocity  $V_{S0}$  [e.g., Tsvankin (1996) and Alkhalifah (1998); a precise analysis is contained in Schoenberg and De Hoop (2000)], such that the influence of  $V_{S0}$  on all kinematic problems involving qP-waves can be ignored. Because we are only dealing with the geometry of map migration, we can for most practical purposes set  $f = 1$  in equations 35, 36, and 53. If  $V_{S0}$  is known,  $f$  can be calculated and subsequently used in equations 35, 36, and 53 to find the phase velocity, its derivative, and the phase angles.

Alkhalifah and Tsvankin (1995) show that the time signatures (e.g., reflection move-out, DMO, and time-migration operators) of qP-waves in homogeneous VTI media are mainly characterized by the zero-dip NMO velocity  $V_{\text{NMO}}(0) = V_{P0} \sqrt{1 + 2\delta}$  and the anellipticity parameter  $\eta = (\epsilon - \delta)/(1 + 2\delta)$ , with an almost negligible influence of  $V_{P0}$ . (To avoid confusion with the NMO velocity at finite dip, we prefer to maintain the notation  $V_{\text{NMO}}(0)$  rather than use  $V_{\text{NMO}}$  as some authors do.) Using these expressions for  $\eta$  and  $V_{\text{NMO}}(0)$ , equations 35 and 36 can, for qP-waves, be rewritten in terms of  $\eta$ ,  $V_{\text{NMO}}(0)$ , and  $V_{P0}$ . The expressions we derive for map migration in VTI media can be used to estimate  $\eta$  and  $V_{\text{NMO}}(0)$  by using the slope information of one event at two (or more) different offsets and calculating the migrated times for these offsets for assumed values of  $\eta$  and  $V_{\text{NMO}}(0)$  (given some  $V_{P0}$ ). The correct values of  $\eta$  and  $V_{\text{NMO}}(0)$  should yield the same migrated time for all offsets since the data have one common reflection point.

### Prestack map time migration

For VTI media, all vertical planes are mirror symmetry planes. Both vertical planes — the one defined by the source position and the reflector position and the one defined by the receiver position and the reflector position — are also symmetry planes. Throughout the remainder of this paper, we refer to these planes as the source and receiver planes (see Figure 1). In the source plane,

$$\tan \psi_s = \frac{\sqrt{(x_s - x_m)^2 + (y_s - y_m)^2}}{z_m}, \quad (37)$$

while in the receiver plane

$$\tan \psi_r = \frac{\sqrt{(x_r - x_m)^2 + (y_r - y_m)^2}}{z_m}, \quad (38)$$

where  $\psi_{s,r}$  are the group angles at the source and receiver and  $z_m$  is the migrated depth. The horizontal slownesses satisfy the relation

$$p_{s,r} = \frac{\sin \theta_{s,r}}{V_{s,r}}, \quad (39)$$

where we define

$$V_{s,r} \equiv V(\theta_{s,r}), \quad (40)$$

$$p_{s,r} \equiv \sqrt{(p_{s,r}^x)^2 + (p_{s,r}^y)^2}, \quad (41)$$

with  $p_{s,r}^{x,y}$  denoting the horizontal slownesses at the source or receiver in the  $x$ - or  $y$ -direction and  $\theta_{s,r}$  as the phase angle at the source or receiver. Using equation 39 in equation 33 and substituting the result in equations 37 and 38, we get

$$\frac{\sqrt{(x_{s,r} - x_m)^2 + (y_{s,r} - y_m)^2}}{z_m} = \frac{V_{s,r} p_{s,r}}{\sqrt{1 - V_{s,r}^2 p_{s,r}^2}} + \frac{1}{V_{s,r}} \frac{dV}{d\theta} \Big|_{s,r} \Big/ \left( 1 - \frac{p_{s,r}}{\sqrt{1 - V_{s,r}^2 p_{s,r}^2}} \frac{dV}{d\theta} \Big|_{s,r} \right). \quad (42)$$

Here,  $(dV/d\theta)|_{s,r}$  is the derivative of the phase velocity with respect to the phase angle  $\theta$  with the vertical symmetry axis, evaluated at the phase angle at the source ( $\theta_s$ ) or receiver ( $\theta_r$ ).

Using equation 42 in equation 34 then results in an expression for the migrated depth:

$$z_m = t_u \left( \frac{1}{V_s \left( \sqrt{1 - V_s^2 p_s^2} - p_s \frac{dV}{d\theta} \Big|_s \right)} + \frac{1}{V_r \left( \sqrt{1 - V_r^2 p_r^2} - p_r \frac{dV}{d\theta} \Big|_r \right)} \right)^{-1}. \quad (43)$$

For pure-mode waves, i.e., qP-qP or qSV-qSV, the migrated depth can be converted to two-way migrated time  $t_m = 2z_m/V_{P0,S0}$ . Defining  $\gamma_{s,r}$  as the angles of the horizontal projection of the slowness vector at the source and receiver with the positive  $x$ -axis see Figure 3, we find

$$\sin \gamma_{s,r} = \frac{y_{s,r} - y_m}{\sqrt{(x_{s,r} - x_m)^2 + (y_{s,r} - y_m)^2}} = \frac{p_{s,r}^y}{p_{s,r}}. \quad (44)$$

Using equation 43 in equation 42 to get an expression for  $\sqrt{(x_{s,r} - x_m)^2 + (y_{s,r} - y_m)^2}$  and substituting the resulting expression in equation 44 then gives

$$y_m = y_{s,r} \frac{t_u p_{s,r}^y \left( V_{s,r} + \sqrt{\frac{1}{V_{s,r}^2 p_{s,r}^2} - 1} \frac{dV}{d\theta} \Big|_{s,r} \right) \left( \sqrt{1 - V_{r,s}^2 p_{r,s}^2} - p_{r,s} \frac{dV}{d\theta} \Big|_{r,s} \right)}{\frac{1}{V_r} \left( \sqrt{1 - V_s^2 p_s^2} - p_s \frac{dV}{d\theta} \Big|_s \right) + \frac{1}{V_s} \left( \sqrt{1 - V_r^2 p_r^2} - p_r \frac{dV}{d\theta} \Big|_r \right)}. \quad (45)$$

The parameters at either the source or the receiver can be used to calculate  $y_m$ , but using the source parameters in the first term of the numerator implies using the receiver parameters in the second term, and vice versa — hence, the order of the subscripts  $s, r$  and  $r, s$ . To find  $x_m$ , we first calculate

$$\cos \gamma_{s,r} = \frac{x_{s,r} - x_m}{\sqrt{(x_{s,r} - x_m)^2 + (y_{s,r} - y_m)^2}} = \frac{p_{s,r}^x}{p_{s,r}}. \quad (46)$$

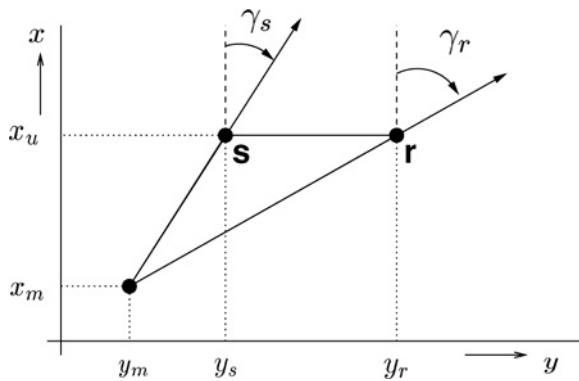


Figure 3. Definition of  $\gamma_{s,r}$  as the angles of the horizontal projections of the slowness vectors with the positive  $x$ -axis.

Using equation 43 again in equation 42 to get an expression for  $\sqrt{(x_{s,r} - x_m)^2 + (y_{s,r} - y_m)^2}$  and using the result in equation 46 gives

$$x_m = x_{s,r} \frac{t_u p_{s,r}^x \left( V_{s,r} + \sqrt{\frac{1}{V_{s,r}^2 p_{s,r}^2} - 1} \frac{dV}{d\theta} \Big|_{s,r} \right) \left( \sqrt{1 - V_{r,s}^2 p_{r,s}^2} - p_{r,s} \frac{dV}{d\theta} \Big|_{r,s} \right)}{\frac{1}{V_r} \left( \sqrt{1 - V_s^2 p_s^2} - p_s \frac{dV}{d\theta} \Big|_s \right) + \frac{1}{V_s} \left( \sqrt{1 - V_r^2 p_r^2} - p_r \frac{dV}{d\theta} \Big|_r \right)}. \quad (47)$$

Again note the order of the subscripts  $s, r$  and  $r, s$ . Thus, equations 43, 45, and 47 are closed-form expressions for the migrated location. The phase velocity and its derivative at the source and receiver in equations 43, 45, and 47 can be set to their respective values for either qP- or qSV-waves, showing the applicability of these expressions for both pure modes and mode-converted waves. The 2D expressions follow by setting  $x_m = x_u = 0$  and  $p_s^x = p_r^x = 0$ .

To find the reflector dip covector  $\xi_m$  (i.e., the wave vector associated with the reflector in the image; see Figure 1b), we use that the slowness vectors  $\mathbf{p}_{s,r}$  obey Snell's law upon reflection at the reflector. Since we define the vertical components of the slowness vectors to point in the negative  $z$ -direction (i.e., upward), we have

$$\xi_m = \xi_s + \xi_r = -\omega(\mathbf{p}_s + \mathbf{p}_r), \quad (48)$$

where  $\omega$  is the angular frequency and  $\xi_{s,r}$  are the wave vectors associated with the source and receiver rays. The slowness vectors at the source and receiver are given by

$$\mathbf{p}_{s,r} = \begin{pmatrix} p_{s,r}^x \\ p_{s,r}^y \\ -\sqrt{\frac{1}{V_{s,r}^2} - p_{s,r}^2} \end{pmatrix}. \quad (49)$$

Therefore, the dip covector  $\xi_m$  is given by

$$\xi_m = \omega \begin{pmatrix} -(p_s^x + p_r^x) \\ -(p_s^y + p_r^y) \\ \sqrt{\frac{1}{V_s^2} - p_s^2} + \sqrt{\frac{1}{V_r^2} - p_r^2} \end{pmatrix}. \quad (50)$$

This expression holds for pure modes and mode-converted waves.

For pure modes,  $\xi_m$  can be translated to the migrated horizontal slowness components  $p_m^{x,y}$  (defining the  $x$ - and  $y$ -components  $v_{x,y}$  of the dip), using

$$-v_{x,y} \equiv \frac{-\xi_m^{x,y}}{\xi_m^z} = \tan \phi_{x,y} = \frac{V_{P0,S0}}{2} \frac{\partial t_m}{\partial (x, y)_m} = V_{P0,S0} p_m^{x,y}, \quad (51)$$

where  $\xi_m^{x,y,z}$  are the components of  $\xi_m$  and  $\phi_{x,y}$  is again the reflector dip with the horizontal in the  $x$ - or  $y$ -direction (measured positive clockwise). Using equation 50 in equation 51, it

follows that

$$p_m^{x,y} = \frac{p_s^{x,y} + p_r^{x,y}}{V_{P0,S0} \left( \sqrt{\frac{1}{V_s^2} - p_s^2} + \sqrt{\frac{1}{V_r^2} - p_r^2} \right)}. \quad (52)$$

Of course, in equations 51 and 52  $V_{P0}$  and  $V_{S0}$  are used for qP-qP- and qSV-qSV-waves, respectively. Again, setting  $x_m = x_u = 0$  and  $p_s^x = p_r^x = 0$  gives the 2D expressions.

### Source and receiver phase angles

Equations 35 and 36 are used to calculate the phase velocity and its derivative, which in turn are used in equations 43, 45, 47, and 50, to find the location and orientation of the reflector in the image. To calculate the phase velocity and its derivative using equations 35 and 36, the angle  $\theta$  and thus  $s = \sin \theta$  need to be known. To find  $s$ , we need to solve equation 39 for  $s$  using equation 35 for the phase velocity. This gives

$$\sin \theta_{s,r} = \left\{ \begin{array}{l} P_{s,r} [(2-f) - 2P_{s,r}(\epsilon - \delta f)] \\ \times \left[ \frac{1 \pm \sqrt{1 - \frac{4(1-f)(1-2\epsilon P_{s,r} - 2P_{s,r}^2 f(\epsilon - \delta))}{(f-2+2P_{s,r}(\epsilon - \delta f))^2}}}{2(1-2\epsilon P_{s,r} - 2P_{s,r}^2 f(\epsilon - \delta))} \right]^{\frac{1}{2}} \end{array} \right\}, \quad (53)$$

where

$$P_{s,r} \equiv p_{s,r}^2 V_{P0}^2, \quad (54)$$

with  $p_{s,r}$  defined in equation 41, the plus sign referring to qP-waves, and the minus sign referring to qSV-waves. Note that for VTI media in two dimensions,  $-\pi/2 < \theta_{s,r} < \pi/2$  and the sign of  $\sin \theta_{s,r}$  is given by the sign of  $p_{s,r}$ ; in this case the right-hand side of equation 53 is preceded by  $\text{sgn}(p_{s,r})$ .

Therefore, given  $V_{P0,S0}$  and the anisotropic parameters  $\epsilon$  and  $\delta$  [or  $\eta$  and  $V_{NMO}(0)$  for qP-waves], we can use equation 53 with the measured  $p_{s,r}$  to calculate the phase angles  $\theta_{s,r}$  for both qP- and qSV-waves. The resulting values can then be used in equations 35 and 36 to find the phase velocity and its derivative at both the source and receiver locations. Note that for the vertical symmetry plane of TTI media, we have  $p = \sin(\nu + \theta)/V(\theta)$ , with  $\nu$  the angle with the vertical of the symmetry axis. In this case we solve numerically for  $\theta$ , provided  $\nu$  is known.

If the horizontal slowness is used to parameterize the phase velocity and its derivative, we need not solve for the phase angles. To find the phase velocity as a function of the horizontal slowness, we replace  $\sin \theta_{s,r}$  with  $V_{s,r} p_{s,r}$  in equation 35 and solve for  $V_{s,r}$ . In Appendix A, we give the resulting expressions for the phase velocity and its derivative as functions of the horizontal slowness for qP-waves, using  $f = 1$  for most practical purposes.

### Zero-offset migration

When we set  $p_s^{x,y} = p_r^{x,y} = p_u^{x,y}$  and  $\theta_s = \theta_r = \theta$ , the prestack map migration equations reduce to their zero-offset counterparts. Here, we treat pure modes only, i.e., we set  $V_s = V_r = V(\theta)$ . Doing this for equations 43, 45, 47, 50, and 52 gives

$$z_m = \frac{V(\theta)t_u}{2} \left( \sqrt{1 - V^2(\theta)p_u^2} - p_u \frac{dV}{d\theta} \Big|_{\theta} \right), \quad (55)$$

$$(x, y)_m = (x, y)_u - \frac{V^2(\theta)p_u^{x,y}t_u}{2} - \frac{V(\theta)p_u^{x,y}t_u}{2} \sqrt{\frac{1}{V^2(\theta)p_u^2} - 1} \frac{dV}{d\theta} \Big|_{\theta}, \quad (56)$$

$$\xi_m = 2\omega \begin{pmatrix} -p_u^x \\ -p_u^y \\ \sqrt{\frac{1}{V^2(\theta)} - p_u^2} \end{pmatrix}, \quad (57)$$

$$p_m^{x,y} = \frac{V(\theta)p_u^{x,y}}{V_{P0,S0}\sqrt{1 - V^2(\theta)p_u^2}}, \quad (58)$$

where  $p_u$  is defined in equation 20. Of course, the migrated depth  $z_m$  can be converted to two-way migrated traveltime  $t_m = 2z_m/V_{P0,S0}$ . Setting  $x_m = x_u = 0$  and  $p_m^x = p_u^x = 0$ , the 2D expressions follow from their 3D counterparts. We can show that the 2D counterparts of equations 55 and 56 for the migrated time and location are equivalent to equation 28 in Cohen (1998). Also, setting  $dV/d\theta = 0$  and replacing  $V(\theta)$  and  $V_{P0}$  with  $v$ , these expressions for VTI media reduce to their counterparts for isotropic media (cf. equations 17–19).

### Prestack map time demigration

For the demigration problem, we assume the migrated location  $(x_m, y_m, z_m)$  and migrated dips  $\phi_{x,y}$  (or  $\nu_{x,y}$ ) are given. To find the unmigrated midpoint location, we need to find the phase angles with the (vertical) symmetry axis and the azimuths of the rays from both the source and the receiver to the reflection point. If we know the angles with the symmetry axis, we can use equations 35, 36, and 39 to find the phase velocity, its derivative, and  $p_{s,r}$ . The projections  $p_{s,r}^{x,y}$  are then calculated using

$$p_{s,r}^x = -\text{sgn}(\nu_x) p_{s,r} \sqrt{1 - (s, r)_\gamma^2}, \quad (59)$$

$$p_{s,r}^y = p_{s,r} (s, r)_\gamma, \quad (60)$$

with  $(s, r)_\gamma = \sin \gamma_{s,r}$ , the azimuth angles  $\gamma_{s,r}$  defined in Figure 3,  $\nu_x$  defined in equation 51, and  $\text{sgn}(\nu_x)$  denoting the sign of  $\nu_x$ . The unmigrated location then follows from solving equations 43, 45, and 47 for  $t_u, y_u$ , and  $x_u$ , using the values for the phase velocity, its derivative, and  $p_{s,r}^{x,y}$ .

To find the azimuth angles  $\gamma_{s,r}$  and the angles with the vertical symmetry axis  $\theta_{s,r}$ , we use the offset and azimuth information and the dips  $\phi_{x,y}$  or  $\nu_{x,y} = -\tan \phi_{x,y}$  (see equation 51). Since in the rotated coordinate system (where the positive  $y$ -axis is in the source-to-receiver direction) the projection onto the  $x$ -axis of the ray connecting the source and the reflector equals the projection of the ray connecting the receiver

and the reflector onto this axis, we must have

$$\begin{aligned} & \frac{\left( s_\theta + \frac{\sqrt{1-s_\theta^2}}{V_s} \frac{dV}{d\theta} \Big|_s \right)}{\sqrt{1-s_\gamma^2} \frac{\left( r_\theta + \frac{\sqrt{1-r_\theta^2}}{V_r} \frac{dV}{d\theta} \Big|_r \right)}{\sqrt{1-r_\theta^2} - \frac{r_\theta}{V_r} \frac{dV}{d\theta} \Big|_r}} \\ &= \sqrt{1-r_\gamma^2} \frac{\left( r_\theta + \frac{\sqrt{1-r_\theta^2}}{V_r} \frac{dV}{d\theta} \Big|_r \right)}{\sqrt{1-r_\theta^2} - \frac{r_\theta}{V_r} \frac{dV}{d\theta} \Big|_r}, \quad (61) \end{aligned}$$

where  $(s, r)_\theta \equiv \sin \theta_{s,r}$  with  $\theta_{s,r}$  the phase angles.

Since  $0 \leq \theta_{s,r} < \pi/2$  and  $0 \leq \gamma_{s,r} < 2\pi$ , we have  $0 \leq (s, r)_\theta < 1$  and  $-1 \leq (s, r)_\gamma \leq 1$ . The azimuth angles vary between 0 and  $2\pi$ , so we need to keep track of the sign of  $\cos \gamma_{s,r}$ . In our rotated coordinate system, the sign of  $v_x$  determines the sign of  $\cos \gamma_{s,r}$ . Therefore, for demigration,

$$\cos \gamma_{s,r} = -\text{sgn}(v_x) \sqrt{1 - (s, r)_\gamma^2}. \quad (62)$$

This also explains the presence of  $\text{sgn}(v_x)$  in equation 59.

Furthermore, the difference of the projections onto the  $y$ -axis should equal the offset  $2h$ , i.e.,

$$\begin{aligned} z_m \left( r_\gamma \frac{\left( r_\theta + \frac{\sqrt{1-r_\theta^2}}{V_r} \frac{dV}{d\theta} \Big|_r \right)}{\sqrt{1-r_\theta^2} - \frac{r_\theta}{V_r} \frac{dV}{d\theta} \Big|_r} \right. \\ \left. - s_\gamma \frac{\left( s_\theta + \frac{\sqrt{1-s_\theta^2}}{V_s} \frac{dV}{d\theta} \Big|_s \right)}{\sqrt{1-s_\theta^2} - \frac{s_\theta}{V_s} \frac{dV}{d\theta} \Big|_s} \right) = 2h. \quad (63) \end{aligned}$$

Using the definitions of  $p_{s,r}^{x,y}$  and equation 50 for  $\xi_m$  in equation 51 for  $v_{x,y}$ , it follows that

$$v_x = \text{sgn}(v_x) \left( \frac{V_r s_\theta \sqrt{1-s_\gamma^2} + V_s r_\theta \sqrt{1-r_\gamma^2}}{V_r \sqrt{1-s_\theta^2} + V_s \sqrt{1-r_\theta^2}} \right), \quad (64)$$

$$v_y = - \left( \frac{V_r s_\theta s_\gamma + V_s r_\theta r_\gamma}{V_r \sqrt{1-s_\theta^2} + V_s \sqrt{1-r_\theta^2}} \right). \quad (65)$$

Equation 61 together with equations 63–65 form a system of four nonlinear equations with four unknowns:  $(s, r)_\theta$  and  $(s, r)_\gamma$ . The phase velocity and its derivative at the source and receiver can be set to their respective values for either qP- or qSV-waves. Hence, these expressions are valid for both pure modes and mode-converted waves. Attempts to eliminate, for example,  $r_\theta$ ,  $s_\gamma$ , and  $r_\gamma$  to get one equation in  $s_\theta$  lead to a high-order polynomial equation in  $s_\theta$ . Therefore, to find the unknown angles, a numerical scheme such as Gauss-Newton (Dennis, 1977) or Levenberg-Marquardt (Moré 1977) might

be used, with the isotropic solution as the initial value. If  $(s, r)_\theta$  and  $(s, r)_\gamma$  are known, the scattering angle can be found using the cosine formula.

In Appendix A, we show that for qP-waves the system of equations 61 and 63–65 can be rewritten into a somewhat simpler system using the horizontal slownesses instead of the phase angles, assuming that for most practical purposes we can set  $f = 1$ . For the 2D problem,  $(s, r)_\gamma = 1$  and  $-1 < (s, r)_\theta < 1$ ; so equations 63 and 65 form a set of two nonlinear equations with two unknowns,  $(s, r)_\theta$ .

### Zero-offset demigration

For zero-offset reflections in homogeneous anisotropic media, the angle of the phase direction with the vertical equals the reflector dip angle; for VTI media the phase angle thus equals this dip angle. Since in the demigration problem this dip is known, we have the phase angle and thus the group angle. Note that in the vertical symmetry plane of TTI media, the reflector dip equals the sum of the phase angle and the tilt of the symmetry axis; for zero-offset demigration in such media, the phase angle is thus also known, provided the tilt of the symmetry axis is known. Therefore, once the position and orientation of the reflector are known, we can calculate the unmigrated location. Here we treat pure modes only.

Using equation 58, we find

$$p_u^2 = \frac{V_{P0,S0}^2 P_m^2}{V^2(\theta) (1 + V_{P0,S0}^2 P_m^2)}, \quad (66)$$

with  $p_m$  defined in equation 31. Using this expression in equation 58, we get

$$p_u^{x,y} = \frac{V_{P0,S0} P_m^{x,y}}{V(\theta) \sqrt{1 + V_{P0,S0}^2 P_m^2}}. \quad (67)$$

To find the two-way traveltime  $t_u$ , we use equation 66 in equation 55 and solve for  $t_u$ . This gives

$$t_u = \frac{2z_m \sqrt{1 + V_{P0,S0}^2 P_m^2}}{\left( V(\theta) - p_m V_{P0,S0} \frac{dV}{d\theta} \Big|_\theta \right)}. \quad (68)$$

Using equations 66–68 in equation 56 gives the unmigrated location,

$$\begin{aligned} (x, y)_u &= (x, y)_m \\ &+ \frac{V_{P0,S0} P_m^{x,y} z_m \left( V(\theta) + \frac{1}{V_{P0,S0} P_m} \frac{dV}{d\theta} \Big|_\theta \right)}{\left( V(\theta) - V_{P0,S0} P_m \frac{dV}{d\theta} \Big|_\theta \right)}. \quad (69) \end{aligned}$$

By setting  $dV/d\theta = 0$  and replacing  $V(\theta)$  and  $V_{P0,S0}$  with the constant velocity  $v$ , the equations for zero-offset demigration in VTI media reduce to their isotropic equivalents (cf. equations 28–30). Also, setting  $x_m = x_u = 0$  and  $p_m^x = p_u^x = 0$  gives the expressions in two dimensions.

Since for zero-offset data in VTI homogeneous media the reflector dip equals the phase angle, we find the phase angle  $\theta$  from

$$\theta = \arctan \sqrt{v_x^2 + v_y^2}. \quad (70)$$

The calculated value of  $\theta$  can subsequently be used in equations 35 and 36 to find the phase velocity and its derivative. Again, we can either use  $V(\theta)$  or  $dV/d\theta|_{\theta}$  for qP- or qSV-waves. For qP-waves we use  $V_{p0}$  in equations 66–69, while for qSV-waves we use  $V_{s0}$ .

### APPLICABILITY OF MAP DEPTH MIGRATION AND DEMIGRATION IN HETEROGENEOUS ANISOTROPIC MEDIA

The closed-form expressions we derived for common-offset and common-azimuth map time migration in homogeneous isotropic media, and for common-azimuth map time migration in VTI media explicitly show that, for a given offset and azimuth, the mapping from the surface measurements (i.e., source and receiver positions, traveltimes, and slopes) to the subsurface image (i.e., reflector position and orientation) is one-to-one for such media (assuming the recorded wavefields reflect only once in the subsurface). Given a scattering angle and azimuth, this mapping exists also in heterogeneous anisotropic media in which caustics can develop, provided that these media do not allow different reflectors to have identical surface seismic measurements that persist under small perturbations of the reflectors. The latter is essentially the Bolker condition (Guillemin, 1985). This mapping defines map depth migration, which allows us to go beyond the framework of normal moveout (NMO). This NMO is the basis of prestack map time migration, making use of rms velocities (treated in the previous sections).

For heterogeneous anisotropic media, the relation between the reflections measured at the surface and the reflectors in the image is, in the high-frequency regime, governed by ray tracing. We capture this relation schematically with the symbol  $\Lambda$ . Since we assume single scattering only, this relation is by definition the canonical relation of the single-scattering modeling or imaging operators that relate the surface seismic measurements to the subsurface image. Map depth migration essentially determines this canonical relation. Throughout the remainder of this paper, we refer to this relation as the canonical relation.

#### Homogeneous isotropic medium case revisited

To clarify the connection between the closed-form expressions for prestack map time migration and demigration derived in the previous sections and the above-mentioned canonical relation, we revisit the isotropic homogeneous medium case. For pure modes (P-P or S-S) in isotropic homogeneous media, the equations determining prestack map time migration using both the horizontal slownesses at the source and receiver follow directly from the equations for homogeneous VTI media by setting  $dV/d\theta = 0$  and  $V_{s,r} = V_{p0,s0} = v$ . Under these restrictions, equations 43, 45, and 47 thus determine the migrated location  $\mathbf{x}_m = (x_m, y_m, z_m)$  for homogeneous isotropic media. Because the expressions for the reflector dip in homogeneous VTI media do not contain the derivative of the phase velocity, the equation for the wavenumber associated with the reflector (or the dip covector)  $\xi_m$  for homogeneous isotropic media is given by equation 50, with  $V_{s,r} = v$ . The canonical relation is now formed by collecting the unmigrated and migrated quantities in a

table, i.e.,

$$\Lambda' = \left\{ \underbrace{(x_u, y_s, y_r, t_u, -\omega(p_s^x + p_r^x), -\omega p_s^y, -\omega p_r^y, \omega)}_{\text{reflection}}; \underbrace{\mathbf{x}_m, \xi_m}_{\text{reflector}} \right\}, \quad (71)$$

where  $\omega$  is the angular frequency. The prime in  $\Lambda'$  indicates that the canonical relation is restricted here to common azimuth. Hence, equations 43, 45, 47, and 50, subject to the restrictions  $dV/d\theta = 0$  and  $V_{s,r} = V_{p0,s0} = v$ , determine the reflector  $(\mathbf{x}_m, \xi_m)$  in the image from the reflections in the data  $(x_u, y_s, y_r, t_u, -\omega(p_s^x + p_r^x), -\omega p_s^y, -\omega p_r^y, \omega)$  and thus define the canonical relation, restricted to common azimuth (i.e.,  $\Lambda'$ ), of the single scattering imaging operator in homogeneous isotropic media. These equations evaluate equation 71 from left to right.

To find the equations determining map time demigration in isotropic homogeneous media, we need to find  $x_u, y_s, y_r, t_u$ , and  $p_{s,r}^{x,y}$  as a function of  $(\mathbf{x}_m, \xi_m)$ . By setting  $dV/d\theta = 0$  and  $V_{s,r} = v$  in equations 61 and 63–65, we get the system of equations that needs to be solved to find the angles  $\theta_{s,r}$  and azimuths  $\gamma_{s,r}$  at the reflector. For pure modes, the resulting system of equations and the solutions for  $(s, r)_{\theta} = (\sin \theta_s, \sin \theta_r)$  and  $(s, r)_{\gamma} = (\sin \gamma_s, \sin \gamma_r)$  are given in Appendix B. Once  $(s, r)_{\theta}$  and  $(s, r)_{\gamma}$  are found, we calculate the source and receiver locations  $(x_u, y_s, y_r)$ , two-way traveltime  $t_u$ , and horizontal slownesses  $p_{s,r}^{x,y}$  from simple geometrical considerations. This gives

$$x_u = x_{s,r} = x_m - \text{sgn}(v_x) \frac{z_m(s, r)_{\theta} \sqrt{1 - (s, r)_{\gamma}^2}}{\sqrt{1 - (s, r)_{\theta}^2}}, \quad (72)$$

$$y_{s,r} = y_m + \frac{z_m(s, r)_{\gamma} (s, r)_{\theta}}{\sqrt{1 - (s, r)_{\theta}^2}}, \quad (73)$$

$$t_u = \frac{z_m}{v} \left( \sqrt{1 - s_{\theta}^2} + \sqrt{1 - r_{\theta}^2} \right), \quad (74)$$

$$p_{s,r}^x = -\text{sgn}(v_x) \sqrt{1 - (s, r)_{\gamma}^2} \frac{(s, r)_{\theta}}{v}, \quad (75)$$

$$p_{s,r}^y = (s, r)_{\gamma} \frac{(s, r)_{\theta}}{v}. \quad (76)$$

These equations determine the reflection in the data  $(x_u, y_s, y_r, t_u, -\omega(p_s^x + p_r^x), -\omega p_s^y, -\omega p_r^y, \omega)$  from the reflector in the image  $(\mathbf{x}_m, \xi_m)$  and thus define the canonical relation, restricted to common azimuth (i.e.,  $\Lambda'$ ), of the single scattering modeling operator in homogeneous isotropic media; they evaluate equation 71 from right to left. Note that equations 21–24 are the common-offset equivalent equations to 72–76.

In the section on map time migration and demigration in isotropic homogeneous media, we show that only the slope in common-offset gathers (as opposed to both common-offset and CMP gathers or common-source and common-receiver gathers) needs to be known to map the surface seismic measurements, restricted to common-offset and common-azimuth geometry to the reflectors in the image. Under these restrictions, the canonical relation for prestack map time migration

is therefore given by

$$\Lambda'' = \left\{ \underbrace{(x_u, y_u - h, y_u + h, t_u, -\omega p_u^x, -\omega p_u^y, \omega)}_{\text{reflection}}; \underbrace{\mathbf{x}_m, \xi_m}_{\text{reflector}} \right\}. \quad (77)$$

Here, the double prime indicates the restriction of the canonical relation to both common offset and common azimuth. Not counting the angular frequency  $\omega$  as a variable, six variables  $(x_u, y_u, t_u, p_u^x, p_u^y, h)$  describe the data. The number of variables  $(\mathbf{x}_m, \xi_m)$  describing the reflector is also six. Hence, for common-offset and common-azimuth data, prestack map time migration and demigration are direct mappings from input to output variables.

### Canonical relation in heterogeneous anisotropic media

Since we derive all expressions for map time migration in the rotated coordinate system with the  $y$ -axis positive in the source-to-receiver direction, these expressions implicitly assume common azimuth, i.e.,  $x_r = x_s = x_u$ . Lifting this restriction, the canonical relation is written as

$$\Lambda = \left\{ \underbrace{(\mathbf{x}_s^h, \mathbf{x}_r^h, t_u, -\omega \mathbf{p}_s^h, -\omega \mathbf{p}_r^h, \omega)}_{\text{reflection}}; \underbrace{\mathbf{x}_m, \xi_m}_{\text{reflector}} \right\}, \quad (78)$$

where  $\mathbf{x}_{s,r}^h = (x_{s,r}, y_{s,r})$  are the source and receiver locations, respectively;  $t_u = t_s + t_r$  is the two-way traveltime;  $\mathbf{p}_{s,r}^h = (p_{s,r}^x, p_{s,r}^y)$  are the horizontal slownesses at the sources and receivers;  $\mathbf{x}_m = (x_m, y_m, z_m)$  is the reflector position in the image; and  $\xi_m = \xi_s + \xi_r$  is the wave vector associated with the reflector. Here, the superscript  $h$  denotes horizontal components only. Note that the vertical components of the slowness vectors  $\mathbf{p}_{s,r}$  are defined to point in the negative  $z$ -direction.

In general media,  $\Lambda$  is evaluated by ray tracing. When we write the solution to the ray-tracing equations, subject to initial conditions  $(\mathbf{x}_0, \xi_0)$  at time 0, in the general form  $(\mathbf{x}(\mathbf{x}_0, \xi_0, t), \xi(\mathbf{x}_0, \xi_0, t))$ , the canonical relation becomes, for a horizontal acquisition surface,

$$\Lambda = \left\{ (\mathbf{x}^h(\mathbf{x}_m, \xi_s, t_s), \mathbf{x}^h(\mathbf{x}_m, \xi_r, t_r), t_u, \xi^h(\mathbf{x}_m, \xi_s, t_s), \xi^h(\mathbf{x}_m, \xi_r, t_r), \omega; \mathbf{x}_m, \xi_s + \xi_r) \right. \\ \left. \text{such that } [z(\mathbf{x}_m, \xi_s, t_s) = 0, z(\mathbf{x}_m, \xi_r, t_r) = 0] \right\},$$

with  $\xi^h \equiv (\xi_x, \xi_y)$ . This symbolically represents a table parameterized by upward ray-tracing from the reflector at location  $\mathbf{x}_m$ .

### Prestack map depth migration and demigration in heterogeneous anisotropic media

Defining  $\mathbf{u} \equiv (x_s, y_s, x_r, y_r, t_u)$  and  $\mathbf{v} \equiv (\omega p_s^x, \omega p_s^y, \omega p_r^x, \omega p_r^y, \omega)$ ,  $(\mathbf{u}, \mathbf{v})$  is a surface seismic measurement characterized by the source and receiver locations, two-way traveltime, and slopes in common source and receiver gathers; it is an element of a phase space  $U$ . Similarly, defining  $\mathbf{m} \equiv \mathbf{x}_m$  and  $\boldsymbol{\mu} \equiv \xi_m$ ,  $(\mathbf{m}, \boldsymbol{\mu})$  describes a reflector defined by its location and orientation in the image; it is an element of a phase space  $M$ .

Let  $P_U$  now denote the projection of  $\Lambda$  on  $U$  and let  $P_M$  denote the projection of  $\Lambda$  on  $M$ . These projections extract, respectively, the surface seismic reflections  $(\mathbf{u}, \mathbf{v})$  and the reflectors in the image  $(\mathbf{m}, \boldsymbol{\mu})$  from the canonical relation  $\Lambda$ , i.e., the table evaluated using ray tracing. Guillemin (1985), in analyzing the generalized Radon transform, introduces the Bolker condition on the canonical relation, which basically states that the medium does not allow different reflectors to have identical surface seismic measurements that persist in being identical under small perturbations of the reflectors, given a velocity model and an acquisition geometry. The Bolker condition is crucial in the development of seismic inverse scattering theory in the presence of caustics (Stolk and de Hoop, 2002a). Here, we explain that this condition can be understood in terms of map migration.

In our application, the Bolker condition reduces to the condition that  $P_U : \Lambda \rightarrow P_U(\Lambda)$  is one-to-one. We can then introduce the mapping  $P_M \circ P_U^{-1} : (\mathbf{u}, \mathbf{v}) \mapsto (\mathbf{m}, \boldsymbol{\mu})$ , which is precisely map depth migration; here,  $\circ$  denotes composition, which can be thought of as a cascade of mappings (i.e.,  $P_U^{-1}$  followed by  $P_M$ ). Hence, the Bolker condition is the condition of applicability of map depth migration in heterogeneous anisotropic media allowing the formation of caustics, given a velocity model and acquisition geometry. In other words, if, given a velocity model and acquisition geometry, one can map depth migrate without ambiguity in either the migrated location or the orientation, then the Bolker condition is satisfied.

Map depth demigration does not require the Bolker condition. To find the surface seismic measurements from a reflector in the image through map depth demigration, we need to specify the scattering angle (for both 2D and 3D seismic measurements) and azimuth (only for 3D seismic measurements) at the reflector, in addition to the reflector location and orientation, i.e.,  $(\mathbf{m}, \boldsymbol{\mu})$ . We introduce these (angle) coordinates by parameterizing the subsets  $\{(\mathbf{m}, \boldsymbol{\mu})\} = \text{constant}$  on  $\Lambda$  and denote them by  $\mathbf{e}$ . Thus,  $(\mathbf{m}, \boldsymbol{\mu}, \mathbf{e})$  form local coordinates on  $\Lambda$ . Map depth demigration then follows from the mapping  $(\mathbf{m}, \boldsymbol{\mu}, \mathbf{e}) \mapsto (\mathbf{u}, \mathbf{v})$ . This mapping is denoted  $\Omega$  in Stolk and de Hoop (2002a). In the absence of caustics,  $\mathbf{e}$  can be chosen to be acquisition offset and azimuth (as in our section on prestack map time demigration in homogeneous VTI media).

## DISCUSSION

We have presented closed-form 3D prestack map time-migration expressions for qP-qP-, qP-qSV-, and qSV-qSV-waves in homogeneous VTI media that specialize to the expressions for P-P-, P-S-, and S-S-waves in homogeneous isotropic media. In addition, we have presented closed-form expressions for prestack map time migration and demigration in the common-offset domain for pure-mode (P-P or S-S) waves in homogeneous isotropic media that use only the slope in the common-offset domain. This provides an additional advantage over methods where both  $p_u$  and  $p_h$  (or, equivalently, both  $p_s$  and  $p_r$ , the slopes at the source and receiver positions) are required, especially since estimating slopes can be cumbersome in the presence of noise. All of the derived prestack expressions reduce properly to their zero-offset counterparts. Our closed-form expressions for prestack map time migration

can be exploited in existing velocity-inversion algorithms that use map migration in such media. In particular, our expressions for prestack map time migration of qP-waves in homogeneous VTI media can be used to determine the anellipticity parameter  $\eta$  (and the zero-dip NMO velocity  $V_{\text{NMO}}(0)$ ) for such media in a time-migration velocity analysis context. For media with mild lateral and vertical velocity variations, our equations can be used provided the velocity is replaced by the local rms velocity. The kinematic equivalence of TI media and orthorhombic media in the symmetry planes generalizes our results for VTI media to these planes in orthorhombic media. In addition, our expressions for VTI media are applicable to the vertical symmetry plane of TTI homogeneous media, which contains the symmetry axis.

Not surprisingly, our closed-form expressions for prestack map time migration in homogeneous isotropic and VTI media exemplify that for such media, given an offset and azimuth, the mapping from the surface seismic measurements (i.e., the source and receiver locations, two-way traveltime, and slopes in common-source and -receiver gathers) to the reflectors in the image (i.e., location and orientation) is one-to-one. We explained that the condition of applicability of prestack map depth migration in heterogeneous anisotropic media that allows the formation of caustics — i.e., that, given a velocity model and acquisition geometry, one can map depth migrate without ambiguity in both the migrated location and orientation — coincides with the Bolker condition for seismic inverse scattering. In addition, we have shown that for homogeneous media, our prestack map time migration and demigration expressions define the canonical relation of the single scattering modeling and imaging operators in such media.

The tangential directions to the recorded wavefronts in seismic data are the directions, locally, in which the data are smooth. Imaging these wavefronts provides the directions in which the medium perturbations are smooth. In mathematical terms, these smooth directions are the wavefront sets of the seismic data and the medium perturbations. In the context of sparsely representing the data and the image, most sparseness (or compression) will be accomplished in the smooth directions, i.e., along the wavefront sets of the data and the medium perturbations. Since, given a scattering angle and azimuth, map migration provides a one-to-one mapping from the singular directions in the data (i.e., the directions normal to the wavefronts) to the singular directions in the image (i.e., the normals to the reflectors), one can thus think of map migration (and demigration) as a mapping between optimally sparse directions. Therefore, it seems that map migration (or demigration) is a suitable vehicle to represent sparsely the imaging (or modeling) operator.

## ACKNOWLEDGMENTS

The authors thank Ken Larner for his critical review of the paper and three anonymous reviewers for their comments that improved the manuscript. H. D. thanks WesternGeco for partial financial support, and Robert Bloor for making him aware of map migration. This work was supported by the sponsors of the Consortium Project on Seismic Inverse Methods for Complex Structures at the Center for Wave Phenomena.

## APPENDIX A

### FROM PHASE ANGLE TO HORIZONTAL SLOWNESS ASSUMING $V_{S0} = 0$

The slowness surface for qP-waves is convex, which, in combination with a VTI medium, ensures that the only branch points in vertical slowness occur at  $\theta = \pm\pi/2$ . In homogeneous media, given the surface seismic geometry, these branch points are never reached, since turning waves do not occur in such media. Thus, for qP-waves in such media, we can parameterize the phase velocity and its derivative uniquely in terms of the horizontal slowness  $p$ .

Substituting  $\sin\theta = pV$  in equation 35 and solving for  $V$  leads to

$$V(p) = V_{P0} \sqrt{\frac{1 + 2p^2 V_{P0}^2 (\delta - \epsilon)}{1 - 2p^2 V_{P0}^2 \epsilon + 2p^4 V_{P0}^4 (\delta - \epsilon)}}, \quad (\text{A-1})$$

where we set  $V_{S0} = 0$  (i.e.,  $f = 1$ ), knowing that the kinematics of qP-waves in anisotropic media are independent of  $V_{S0}$  within the limits of seismic accuracy (Alkhalifah, 1998). The derivative  $dV/dp$  is then

$$\frac{dV}{dp} = \frac{2p V_{P0}^3 \delta - 4p^3 V_{P0}^5 (\delta - \epsilon) - 4p^5 V_{P0}^7 (\delta - \epsilon)^2}{(1 - 2p^2 V_{P0}^2 \epsilon + 2p^4 V_{P0}^4 (\delta - \epsilon))^{3/2} \sqrt{1 + 2p^2 V_{P0}^2 (\delta - \epsilon)}}. \quad (\text{A-2})$$

Note that both expressions can be readily rewritten in terms of  $\eta$ ,  $V_{\text{NMO}}(0)$ , and  $V_{P0}$ .

Using these expressions, we can write the vertical slowness  $q = \sqrt{1/V^2 - p^2}$  as

$$q = \frac{1}{V_{P0}} \sqrt{\frac{1 - p^2 V_{P0}^2 (1 + 2\epsilon)}{1 + 2p^2 V_{P0}^2 (\delta - \epsilon)}} \quad (\text{A-3})$$

or, in terms of  $\eta$ ,  $V_{\text{NMO}}(0)$ , and  $V_{P0}$  [see also Alkhalifah (1998, his equation A-10)],

$$q = \frac{1}{V_{P0}} \sqrt{1 - \frac{p^2 V_{\text{NMO}}^2(0)}{1 - 2p^2 V_{\text{NMO}}^2(0)\eta}}. \quad (\text{A-4})$$

To calculate the group angle (see equation 33) as a function of the horizontal slowness, we use the chain rule,

$$\frac{dV}{d\theta} = \frac{dV}{dp} \frac{dp}{d\theta}. \quad (\text{A-5})$$

Using  $p = \sin\theta/V$ , this becomes

$$\frac{dV}{d\theta} = \frac{\left(\frac{dV}{dp} \sqrt{1 - p^2 V^2}\right)}{\left(V + p \frac{dV}{dp}\right)}, \quad (\text{A-6})$$

where we use  $\cos(\theta) = \sqrt{1 - p^2 V^2} > 0$  in homogeneous VTI media. This expression together with equations A-1 and A-2 in equation 33 results in

$$\tan\psi = \frac{p V_{P0} (1 + 2\delta)}{(1 + 2p^2 V_{P0}^2 (\delta - \epsilon))^{3/2} \sqrt{1 - p^2 V_{P0}^2 (1 + 2\epsilon)}}, \quad (\text{A-7})$$

or, in terms of  $\eta$ ,  $V_{\text{NMO}}(0)$ , and  $V_{p0}$ ,

$$\begin{aligned} \tan \psi &= \frac{pV_{\text{NMO}}^2(0)}{V_{p0} (1 - 2p^2V_{\text{NMO}}^2(0)\eta)^{3/2} \sqrt{1 - p^2V_{\text{NMO}}^2(0)(1 + 2\eta)}}. \end{aligned} \quad (\text{A-8})$$

Using the simplified expressions A-4 and A-8 for the vertical slowness and group angle in equations 61 and 63–65 leads to the following system of equations for prestack map demigration in homogeneous VTI media:

$$\begin{aligned} 0 &= \frac{p_s \sqrt{1 - s_\gamma^2}}{(1 - 2\eta p_s^2 V_{\text{NMO}}^2(0))^{3/2} \sqrt{1 - p_s^2 V_{\text{NMO}}^2(0)(1 + 2\eta)}} \\ &\quad - \frac{p_r \sqrt{1 - r_\gamma^2}}{(1 - 2\eta p_r^2 V_{\text{NMO}}^2(0))^{3/2} \sqrt{1 - p_r^2 V_{\text{NMO}}^2(0)(1 + 2\eta)}}, \end{aligned} \quad (\text{A-9})$$

$$\begin{aligned} \frac{4h}{V_{\text{NMO}}^2(0)} &= \frac{t_m r_\gamma p_r}{(1 - 2\eta p_r^2 V_{\text{NMO}}^2(0))^{3/2} \sqrt{1 - p_r^2 V_{\text{NMO}}^2(0)(1 + 2\eta)}} \\ &\quad - \frac{t_m s_\gamma p_s}{(1 - 2\eta p_s^2 V_{\text{NMO}}^2(0))^{3/2} \sqrt{1 - p_s^2 V_{\text{NMO}}^2(0)(1 + 2\eta)}}, \end{aligned} \quad (\text{A-10})$$

$$\begin{aligned} v_x &= \frac{\text{sgn}(v_x) V_{p0} (p_s \sqrt{1 - s_\gamma^2} + p_r \sqrt{1 - r_\gamma^2})}{\sqrt{1 - \frac{p_s^2 V_{\text{NMO}}^2(0)}{1 - 2\eta p_s^2 V_{\text{NMO}}^2(0)}} + \sqrt{1 - \frac{p_r^2 V_{\text{NMO}}^2(0)}{1 - 2\eta p_r^2 V_{\text{NMO}}^2(0)}}}, \end{aligned} \quad (\text{A-11})$$

$$\begin{aligned} v_y &= - \frac{V_{p0}(s_\gamma p_s + r_\gamma p_r)}{\sqrt{1 - \frac{p_s^2 V_{\text{NMO}}^2(0)}{1 - 2\eta p_s^2 V_{\text{NMO}}^2(0)}} + \sqrt{1 - \frac{p_r^2 V_{\text{NMO}}^2(0)}{1 - 2\eta p_r^2 V_{\text{NMO}}^2(0)}}}. \end{aligned} \quad (\text{A-12})$$

For the 2D problem we have  $(s, r)_\gamma = 1$  and  $-1 < (s, r)_\theta = V_{s,r} p_{s,r} < 1$ . Equations A-10 and A-12 then form a nonlinear system of two equations with two unknowns — namely,  $p_s$  and  $p_r$ .

## APPENDIX B

### SOLVING FOR SCATTERING ANGLE AND AZIMUTH FOR PRESTACK DEMIGRATION IN HOMOGENEOUS ISOTROPIC MEDIA

To find the angles  $\theta_{s,r}$  (see Figure 1a) and azimuths  $\gamma_{s,r}$  (see Figure 3) for prestack demigration of pure-mode (P-P or S-S) waves in homogeneous isotropic media, we set  $dV/d\theta = 0$  and  $V_s = V_r = V_{p0} = v$  in equations 61, 63–65. The resulting system of equations is

$$\sqrt{1 - s_\gamma^2} \frac{s_\theta}{\sqrt{1 - s_\theta^2}} = \sqrt{1 - r_\gamma^2} \frac{r_\theta}{\sqrt{1 - r_\theta^2}}, \quad (\text{B-1})$$

$$\left( r_\gamma \frac{r_\theta}{\sqrt{1 - r_\theta^2}} - s_\gamma \frac{s_\theta}{\sqrt{1 - s_\theta^2}} \right) = \frac{4h}{vt_m}, \quad (\text{B-2})$$

$$\text{sgn}(v_x) \left( \frac{s_\theta \sqrt{1 - s_\gamma^2} + r_\theta \sqrt{1 - r_\gamma^2}}{\sqrt{1 - s_\theta^2} + \sqrt{1 - r_\theta^2}} \right) = v_x, \quad (\text{B-3})$$

$$- \left( \frac{s_\theta s_\gamma + r_\theta r_\gamma}{\sqrt{1 - s_\theta^2} + \sqrt{1 - r_\theta^2}} \right) = v_y, \quad (\text{B-4})$$

where  $(s, r)_\theta = (\sin \theta_s, \sin \theta_r)$  and  $(s, r)_\gamma = (\sin \gamma_s, \sin \gamma_r)$  are unknown. (From these equations it is clear that the cases  $(s, r)_\theta = 1$ , i.e., 90° dipping reflectors, are not included in this system of equations. By choosing  $0 \leq \theta < \pi/2$ , we exclude these impractical cases.)

To find  $s_\theta$ , we first use equations B-2 and B-4 to eliminate  $r_\theta r_\gamma$ . Then we eliminate  $s_\theta \sqrt{1 - s_\gamma^2}$  from equations B-1 and B-3 and combine the results to give an equation with only  $s_\theta$ ,  $s_\gamma$ , and  $r_\gamma$ :

$$\begin{aligned} &\left( \frac{v_x vt_m}{2} \right)^2 \left\{ v_y \sqrt{1 - s_\theta^2} + s_\theta s_\gamma \right\}^2 \\ &= (1 - r_\gamma^2) \left\{ 4h^2 + 2hvt_m \left( v_y + \frac{s_\theta s_\gamma}{\sqrt{1 - s_\theta^2}} \right) \right. \\ &\quad \left. + \left( \frac{s_\theta vt_m}{2} \right)^2 \left( v_y + \frac{s_\theta s_\gamma}{\sqrt{1 - s_\theta^2}} \right)^2 \right\}. \end{aligned} \quad (\text{B-5})$$

To get  $r_\gamma^2$  as a function of  $s_\theta$  and  $s_\gamma$ , we use equations B-1 and B-2 to eliminate  $r_\theta/\sqrt{1 - r_\theta^2}$  and subsequently solve for  $r_\gamma^2$ . This gives

$$\begin{aligned} r_\gamma^2 &= \frac{\left( 2h \sqrt{1 - s_\theta^2} + \frac{s_\theta s_\gamma vt_m}{2} \right)^2}{4h^2 (1 - s_\theta^2) + 2hs_\theta s_\gamma vt_m \sqrt{1 - s_\theta^2} + \left( \frac{s_\theta vt_m}{2} \right)^2}. \end{aligned} \quad (\text{B-6})$$

Before we substitute this expression for  $r_\gamma^2$  into equation B-5, we first eliminate  $r_\theta \sqrt{1 - r_\gamma^2}$  from equations B-1 and B-3, and solve for  $s_\gamma^2$ , which gives

$$s_\gamma^2 = 1 + v_x^2 - \frac{v_x^2}{s_\theta^2}, \quad (\text{B-7})$$

where  $s_\theta \neq 0$ . Then, using equations B-6 and B-7 in equation B-5 gives

$$\begin{aligned} &(1 - s_\theta^2) \{ h^2 [\beta (1 - s_\theta^2) - 4v_y^2] + 2v_y h \alpha \} \\ &= \frac{v_x^2 t_m^2}{4} \{ \beta [(1 + 2v_x^2) s_\theta^2 - (1 + v_x^2) s_\theta^4 - v_x^2] - v_y^2 \}, \end{aligned} \quad (\text{B-8})$$

with  $v_x \neq 0$  and where we define

$$\alpha \equiv \frac{vt_m}{2} (1 + v_x^2 - v_y^2), \quad (\text{B-9})$$

$$\beta \equiv (1 + v_x^2 + v_y^2)^2. \quad (\text{B-10})$$

Note that the special case  $v_x = 0$  is really equivalent to the 2D case treated below. Equation B-8 is a quadratic equation in  $s_\theta^2$  that can be solved for  $s_\theta$  to give

$$s_\theta = \sqrt{\frac{2h^2(\beta - 2v_y^2) + 2v_y h(\alpha \pm \gamma) + \left[\beta \left(\frac{vt_m}{2}\right)^2 (1 + 2v_x^2) \mp \alpha\gamma\right]}{2\beta \left(h^2 + (1 + v_x^2) \left(\frac{vt_m}{2}\right)^2\right)}} \quad (\text{B-11})$$

with

$$\gamma \equiv \sqrt{4v_y^2 h^2 + \beta \left(\frac{vt_m}{2}\right)^2} \quad (\text{B-12})$$

The proper root in equation B-11 is then found through substitution in the original system of equations B-1–B-4.

Once  $s_\theta$  is found, we need to solve for the remaining parameters  $r_\theta$  and  $(s, r)_\gamma$ . To find  $r_\theta$  we first use equation B-4 in equation B-2 to eliminate  $r_\theta r_\gamma$  to give

$$-\frac{4h}{vt_m} = v_y + \frac{v_y \sqrt{1 - s_\theta^2}}{\sqrt{1 - r_\theta^2}} + s_\theta s_\gamma \left( \frac{1}{\sqrt{1 - s_\theta^2}} + \frac{1}{\sqrt{1 - r_\theta^2}} \right) \quad (\text{B-13})$$

To eliminate  $s_\gamma$  we use equation B-7 and subsequently solve for  $r_\theta$  to give

$$r_\theta = \sqrt{1 - \left( \frac{hvt_m \sqrt{s_\theta^2 - v_x^2(1 - s_\theta^2)} - \sqrt{1 - s_\theta^2} [v_y hvt_m + \Delta]}{4h^2 + 2v_y hvt_m + \Delta} \right)^2} \quad (\text{B-14})$$

where we define

$$\Delta \equiv \frac{v^2 t_m^2}{4} \left( v_x^2 + v_y^2 - \frac{s_\theta^2}{1 - s_\theta^2} \right).$$

Once  $(s, r)_\theta$  are found, we solve equation B-13 for  $s_\gamma$  to get

$$s_\gamma = -\frac{\sqrt{1 - s_\theta^2} \left( v_y \sqrt{1 - s_\theta^2} + \sqrt{1 - r_\theta^2} \left( \frac{4h}{vt_m} + v_y \right) \right)}{s_\theta \left( \sqrt{1 - s_\theta^2} + \sqrt{1 - r_\theta^2} \right)} \quad (\text{B-15})$$

provided  $s_\theta \neq 0$ . Finally, using equation B-4 in equation B-2 to eliminate  $s_\gamma s_\theta$  and solving for  $r_\gamma$ , we find

$$r_\gamma = \frac{\sqrt{1 - r_\theta^2} \left( \sqrt{1 - s_\theta^2} \left( \frac{4h}{vt_m} - v_y \right) - v_y \sqrt{1 - r_\theta^2} \right)}{r_\theta \left( \sqrt{1 - s_\theta^2} + \sqrt{1 - r_\theta^2} \right)} \quad (\text{B-16})$$

provided  $r_\theta \neq 0$ .

### Special cases

In two dimensions, the system of equations B-1–B-4 reduces to two equations with two unknowns:

$$\left( \frac{r_\theta}{\sqrt{1 - r_\theta^2}} - \frac{s_\theta}{\sqrt{1 - s_\theta^2}} \right) = \frac{4h}{vt_m} \quad (\text{B-17})$$

$$- \left( \frac{s_\theta + r_\theta}{\sqrt{1 - s_\theta^2} + \sqrt{1 - r_\theta^2}} \right) = v_y \quad (\text{B-18})$$

with  $-1 < (s, r)_\theta < 1$ . To solve this system for the unknowns  $(s, r)_\theta$ , we first rewrite equation B-17 to get

$$\sqrt{1 - r_\theta^2} = \frac{r_\theta vt_m \sqrt{1 - s_\theta^2}}{4h \sqrt{1 - s_\theta^2} + s_\theta vt_m} \quad (\text{B-19})$$

Using this expression in equation B-18 to eliminate  $\sqrt{1 - r_\theta^2}$  then gives

$$r_\theta = - \left( s_\theta + \frac{4v_y h (1 - s_\theta^2)}{s_\theta vt_m + \sqrt{1 - s_\theta^2} (4h + v_y vt_m)} \right) \quad (\text{B-20})$$

Using equation B-19 to calculate  $1/r_\theta^2 = (\sqrt{1 - r_\theta^2}/r_\theta)^2 + 1$  and multiplying the result with  $r_\theta^2$  calculated using equation B-20 gives

$$\begin{aligned} & \left( \left[ 4h \sqrt{1 - s_\theta^2} + s_\theta vt_m \right]^2 + [1 - s_\theta^2] v^2 t_m^2 \right) \left( 4h v_y [1 - s_\theta^2] \right. \\ & \quad \left. + s_\theta^2 vt_m + s_\theta \sqrt{1 - s_\theta^2} [4h + v_y vt_m] \right)^2 \\ & = \left( 4h \sqrt{1 - s_\theta^2} + s_\theta vt_m \right)^2 \left( s_\theta vt_m \right. \\ & \quad \left. + \sqrt{1 - s_\theta^2} [4h + v_y vt_m] \right)^2 \quad (\text{B-21}) \end{aligned}$$

Dividing both sides of this expression by  $(1 - s_\theta^2)(4h \sqrt{1 - s_\theta^2} + s_\theta vt_m)^2$  and simplifying the result gives a quadratic equation in  $\tan \theta_s = s_\theta / \sqrt{1 - s_\theta^2} \equiv \tau_{\theta s}$ , namely,

$$\begin{aligned} & v_y vt_m \tau_{\theta s}^2 + (4h v_y + vt_m (v_y^2 - 1)) \tau_{\theta s} \\ & \quad + 2h (v_y^2 - 1) - v_y vt_m = 0, \quad (\text{B-22}) \end{aligned}$$

with roots

$$\tau_{\theta s} = \frac{1}{2v_y} (1 - v_y^2) - \frac{2h}{vt_m} \pm \sqrt{\frac{4h^2}{v^2 t_m^2} + \frac{(1 + v_y^2)^2}{4v_y^2}} \quad (\text{B-23})$$

By using this expression in equation B-17, we find

$$\tau_{\theta r} = \frac{1}{2v_y} (1 - v_y^2) + \frac{2h}{vt_m} \pm \sqrt{\frac{4h^2}{v^2 t_m^2} + \frac{(1 + v_y^2)^2}{4v_y^2}} \quad (\text{B-24})$$

with  $\tau_{\theta r} \equiv \tan \theta_r = r_\theta / \sqrt{1 - r_\theta^2}$ . Therefore,  $(s, r)_\theta$  are then given by

$$(s, r)_\theta = \sin(\arctan(\tau_{\theta s}, \tau_{\theta r})). \quad (\text{B-25})$$

The proper roots in equations B-23 and B-24 are then chosen through substitution in the original system of equations B-17

and B-18. Note that the cases  $(s, r)_\theta = 0$  mentioned in the previous subsection are included in this solution.

For the special case  $v_y = 0$ , i.e., the 2D zero dip case, the solution for  $(s, r)_\theta$  is given by

$$s_\theta = \sin \left( \arctan \left( \frac{-2h}{vt_m} \right) \right) = -r_\theta. \quad (\text{B-26})$$

## REFERENCES

- Alkhalifah, T., 1996, Seismic processing in transversely isotropic media: PhD thesis, Colorado School of Mines.
- , 1998, Acoustic approximations for processing in transversely isotropic media: *Geophysics*, **63**, 623–631.
- Alkhalifah, T., and I. Tsvankin, 1995, Velocity analysis for transversely isotropic media: *Geophysics*, **60**, 1550–1566.
- Billette, F., and G. Lambaré, 1998, Velocity macro-model estimation from seismic reflection data by stereotomography: *Geophysical Journal International*, **135**, 671–690.
- Bishop, T., K. Bube, R. Cutler, R. Langan, P. Love, J. Résnick, R. Shuey, D. Spindler, and H. Wyld, 1985, Tomographic determination of velocity and depth in laterally varying media: *Geophysics*, **50**, 903–923.
- Červený, V., 2001, *Seismic ray theory*: Cambridge University Press.
- Claerbout, J. F., 1985, *Imaging the earth's interior*: Blackwell Scientific Publications.
- Cohen, J. K., 1998, A convenient expression for the NMO velocity function in terms of ray parameter: *Geophysics*, **63**, 275–278.
- De Hoop, M. V., and S. Brandsberg-Dahl, 2000, Maslov asymptotic extension of generalized Radon transform inversion in anisotropic elastic media: A least-squares approach: *Inverse Problems*, **16**, 519–562.
- Dennis, J. J., 1977, Nonlinear least squares, in D. Jacobs, ed., *State of the art in numerical analysis*: Academic Press, 269–312.
- Gjoystdal, H., and B. Ursin, 1981, Inversion of reflection times in three dimensions: *Geophysics*, **46**, 972–983.
- Graeser, E., W. Lode, and G. Pott, 1957, Representation of depth-contour maps of arbitrarily curved reflection horizons, including refraction of rays, three-dimensional case: *Geophysical Prospecting*, **5**, 135–141.
- Gray, W., and J. Golden, 1983, Velocity determination in a complex earth: 53rd Annual International Meeting, SEG, Expanded Abstracts, 577–579.
- Guillemin, V., 1985, On some results of Gelfand in integral geometry: *Proceedings of Symposia in Pure Mathematics*, **43**, 149–155.
- Haas, A., and J. Viallix, 1976, Krigeage applied to geophysics: *Geophysical Prospecting*, **24**, 49–69.
- Harlan, W., and R. Burridge, 1983, A tomographic velocity inversion for unstacked data: Stanford Exploration Project report SEP-37, 1–7.
- Hermont, A., 1979, Letter to the editor, re: Seismic controllable directional reception as practiced in the USSR: *Geophysics*, **44**, 1601–1602.
- Iversen, E., and H. Gjoystdal, 1996, Event-oriented velocity estimation based on prestack data in time or depth domain: *Geophysical Prospecting*, **44**, 643–686.
- Iversen, E., H. Gjoystdal, and J. Hansen, 2000, Prestack map migration as an engine for parameter estimation in TI media: 70th Annual International Meeting, SEG, Expanded Abstracts, 1004–1007.
- Kleyn, A., 1977, On the migration of reflection time contour maps: *Geophysical Prospecting*, **25**, 125–140.
- Maher, S., and D. Hadley, 1985, Development of an accurate, stable, and interactive map migration algorithm: 55th Annual International Meeting, SEG, Expanded Abstracts, 551–552.
- Maher, S., J. Thorson, D. Hadley, and H. Swanger, 1987, Study of comparative interval velocities for map migration: 57th Annual International Meeting, SEG, Expanded Abstracts, 471–473.
- More, J., 1977, The Levenberg-Marquardt algorithm: Implementation and theory, in G. Watson, ed., *Numerical analysis lecture notes in mathematics* 630: Springer Verlag, 105–116.
- Musgrave, A., 1961, Wave-front charts and three-dimensional migrations: *Geophysics*, **26**, 738–753.
- Reilly, J., 1991, Integrated interpretation, 3D map migration and VSP modelling project, northern U.K. southern gas basin: *Geophysical Prospecting*, **39**, 253–278.
- Riabinkin, L., 1991, Fundamentals of resolving power of controlled directional reception (CDR) of seismic waves, in G. Gardner, and L. Lu, eds., *Slant stack processing*: Society of Exploration Geophysicists, 36–60.
- Rieber, F., 1936, A new reflection system with controlled directional sensitivity: *Geophysics*, **1**, 97–106.
- Sattlegger, J., 1964, Series for three-dimensional migration in reflection seismic interpretation: *Geophysical Prospecting*, **12**, 115–134.
- Sattlegger, J., P. Stiller, J. Echterhoff, and M. Hentschke, 1980, Common offset plane migration: *Geophysical Prospecting*, **28**, 859–871.
- Schoenberg, M. A., and M. de Hoop, 2000, Approximate dispersion relations for qP-qSV waves in transversely isotropic media: *Geophysics*, **65**, 919–933.
- Stolk, C. C., and M. V. de Hoop, 2001, Seismic inverse scattering in the 'wave-equation' approach: MSRI preprint 2001-047, <http://www.msri.org/publications/preprints/online/2001-047.html>.
- , 2002, Microlocal analysis of seismic inverse scattering in anisotropic, elastic media: *Communications in Pure and Applied Mathematics*, **55**, 261–301.
- Sword, C. H., 1987, Tomographic determination of interval velocities from reflection seismic data: The method of controlled directional reception: PhD thesis, Stanford University.
- ten Kroode, A., D.-J. Smit, and A. R. Verdel, 1998, A microlocal analysis of migration: *Wave Motion*, **28**, 149–172.
- Thomsen, L., 1986, Weak elastic anisotropy: *Geophysics*, **51**, 1954–1966.
- Tsvankin, I., 1996, P-wave signatures and notation for transversely isotropic media: An overview: *Geophysics*, **61**, 467–483.
- , 2001, Seismic signatures and analysis of reflection data in anisotropic media: Elsevier Science Publishing Co., Ltd.
- van Trier, J., 1990, Tomographic determination of structural velocities from depth-migrated seismic data: PhD thesis, Stanford University.
- Weber, M., 1955, Die bestimmung einer beliebig gekrueemten schichtgrenze aus seismischen reflexionsmessungen: *Geofisica Pura e Applicata*, **32**, 7–11.
- Whitcombe, D., and R. Carroll, 1994, The application of map migration to 2-D migrated data: *Geophysics*, **59**, 1121–1132.
- Zavalishin, B., 1981, Perfection of methods for constructing seismic images using controlled directional reception: *Soviet Geology and Geophysics*, **22**, 98–104.